DEC 23 1946

NATIONAL ADVISORY COMMITTEE FOR AERONAUTICS

WARTIME REPORT

ORIGINALLY ISSUED

October 1944 as
Advance Restricted Report L4I11f

WIND-TUNNEL INVESTIGATION OF CONTROL-SURFACE CHARACTERISTICS

XX - PLAIN AND BALANCED FLAPS ON AN NACA 0009 RECTANGULAR SEMISPAN TAIL SURFACE

By I. Elizabeth Garner

Langley Memorial Aeronautical Laboratory
Langley Field, Va.

FOR REFERENCE

NOT TO BE TAKEN FROM THIS ROOM

NACA

WASHINGTON

NACA LIBRARY
LANGLEY MEMORIAL AERONAUTICAL
LABORATORY
Langley Field, Va.

NACA WARTIME REPORTS are reprints of papers originally issued to provide rapid distribution of advance research results to an authorized group requiring them for the war effort. They were previously held under a security status but are now unclassified. Some of these reports were not technically edited. All have been reproduced without change in order to expedite general distribution.

3 1176 01363 8946

NACA ARR No. L4I11f

NATIONAL ADVISORY COMMITTEE FOR AERONAUTICS

ADVANCE RESTRICTED REPORT

WIND-TUNNEL INVESTIGATION OF CONTROL-SURFACE CHARACTERISTICS

XX - PLAIN AND BALANCED FLAPS ON AN NACA 0009 RECTANGULAR SEMISPAN TAIL SURFACE

By I. Elizabeth Garner

SUMMARY

Force-test measurements have been made in the Langley 4- by 6-foot vertical tunnel to determine the aerodynamic characteristics of an NACA 0009 semispan tail surface of rectangular plan form equipped with flaps of various nose shapes and overhangs. The flap chord was 30 percent of the airfoil chord. A few tests were made to determine the effectiveness of a balancing tab on various flap arrangements.

The test results indicated that the slope of the lift curve was affected little by the amount of overhang and the balance nose shape but was increased by sealing the gap at the flap nose. At zero angle of attack, the variation of lift with flap deflection for the sealed-gap condition was the same as or slightly greater than for the unsealed-gap condition. The change in the hinge-moment coefficient with angle of attack or with flap deflection generally was made more negative with sealing the gap. The effectiveness of the balancing tab in reducing the flap hinge-moment coefficients was approximately the same for both the sealed plain flap and the unsealed 35-percent-flap-chord elliptical overhang; also, the variation of lift coefficient with tab deflection was about equal for the plain flap and for the flap with aerodynamic balance.

In three-dimensional flow, the measured values of the lift-curve slope were slightly lower and the measured values of the hinge-moment parameters were more positive than the values of the parameters calculated from the data of previous investigations in two-dimensional flow by lifting-line theory, modified by the edge-velocity correction. Application of aspect-ratio corrections

determined from a lifting-surface-theory solution for an elliptical wing made the computed values of the variation of the hinge-moment coefficient with angle of attack very closely approach the measured values.

INTRODUCTION

The NACA is conducting an extensive investigation of the aerodynamic characteristics of control surfaces in two-dimensional and three-dimensional flow in order to provide design data and to determine flap arrangements suitable for use as control surfaces. A series of tests has been made to determine the effects of overhang, nose shape, and gap on the aerodynamic characteristics of an NACA 0009 airfoil in two-dimensional flow; the results are presented in references 1 to 4 and summarized in reference 5.

The present investigation consisted of tests in three-dimensional flow of an NACA 0009 rectangular semi-span tail surface. The purpose of this investigation was to help establish a correlation between aerodynamic characteristics in two-dimensional and three-dimensional flow. Through the use of a surface having constant airfoil, flap, and balance chords, only relatively simple planform corrections were required when approximate corrections were used.

SYMBOLS

The coefficients and the symbols used in this paper are defined as follows:

C_L lift coefficient (L/qS)

C_D drag coefficient (D/qS)

C_m pitching-moment coefficient about 0.35c axis (M/qSc)

C_{h_f} flap hinge-moment coefficient $\left(H_f/q\overline{c_f}^2 b_f\right)$

where

L	twice lift of semispan model
D	twice drag of semispan model
M	twice pitching moment of semispan model
H_f	twice flap hinge moment of semispan model
q	dynamic pressure $\left(\frac{1}{2}\rho V^2\right)$
S	twice area of semispan model
b_f	twice flap span of semispan model
c	chord of airfoil with flap and tab neutral
$\overline{c_f}$	root-mean-square chord of flap
ρ	mass density of air
V	velocity

and

A	aspect ratio
b	twice span of semispan model
c_f	chord of flap
c_b	chord of overhang
α	angle of attack of model
δ_f	flap deflection relative to airfoil; positive when trailing edge is deflected downward
δ_t	tab deflection relative to flap; positive when trailing edge is deflected downward
k	constant used in determining jet-boundary hinge-moment correction
E	edge-velocity correction factor (see reference 6)

$$c_{L_\alpha} = \left(\frac{\partial C_L}{\partial \alpha}\right)_{\delta_f}$$

$$\alpha_{\delta_f} = \left(\frac{\partial \alpha}{\partial \delta_f}\right)_{C_L}$$

$$c_{h_{f_\alpha}} = \left(\frac{\partial C_{h_f}}{\partial \alpha}\right)_{\delta_f}$$

$$c_{h_{f_{\delta_f}}} = \left(\frac{\partial C_{h_f}}{\partial \delta_f}\right)_{\alpha}$$

$$c_{h_{f_{\delta_t}}} = \left(\frac{\partial C_{h_f}}{\partial \delta_t}\right)_{\alpha,\delta_f}$$

$$\left(C_{m_{C_L}}\right)_{\delta_f} = \left(\frac{\partial C_m}{\partial C_L}\right)_{\delta_f}$$

$$\left(C_{m_{C_L}}\right)_{\alpha} = \left(\frac{\partial C_m}{\partial C_L}\right)_{\alpha}$$

The subscript outside the parentheses indicates the factor held constant in determining the parameter.

APPARATUS, MODEL, AND TESTS

The tests were made in the Langley 4- by 6-foot vertical tunnel (reference 7) modified as discussed in reference 2. The 2-foot-chord by 3-foot-semispan model was made of laminated mahogany and conformed to the dimensions of figure 1 and to the NACA 0009 profile, the stations and ordinates of which are given in table I. Since the tail surface had a tip of revolution, the tip plan form was the same as the contour of the upper and lower surfaces of the airfoil. The flap chord was 30 percent of the airfoil chord at each spanwise station. For the complete tail surface represented by the semispan model, the aspect ratio was 3 and the taper ratio, 1.

The plain unbalanced flap and the flaps with overhang balance are shown in figure 1. The $0.35c_f$ and $0.50c_f$ overhangs were tested with blunt and elliptical nose shapes. (See fig. 1 and table II.) The elliptical nose was a true ellipse faired tangent to the airfoil contour at the hinge axis. The gap was fixed at 0.005c and for some tests was sealed with a sheet-rubber seal.

A linked balancing tab constructed of brass and having a gap of 0.001c was tested on the plain sealed flap and on the flap with $0.35c_f$ elliptical overhang with open gap. The tab had a chord of $0.20c_f$ (fig. 1) and a span 50 percent of the flap semispan. The ratio of the tab deflection to the flap deflection was -1:1.

The rectangular tail surface was tested as a semispan model by mounting it horizontally in the tunnel with the inboard end adjacent to the wall of the tunnel, which thereby acted as a reflection plane (fig. 2). The model was supported entirely by the balance frame with a small clearance at the tunnel wall so that all forces and moments acting on the model could be measured. The flow over the model simulated the flow over the right semispan of a complete tail surface consisting of the test panel and its reflection mounted in an 8- by 6-foot wind tunnel. The flap hinge moments were obtained by measuring the amount of twist in a long flexible torque tube, one end of which was attached to the flap by means of a linkage arrangement and the other end of which extended outside the tunnel to a calibrated dial.

The tests were made at a dynamic pressure of 15 pounds per square foot, which corresponds to an air velocity of about 76 miles per hour at standard sea-level conditions. The test Reynolds number was 1,430,000 and the effective Reynolds number of the tests was approximately 2,760,000. (Effective Reynolds number = Test Reynolds number × Turbulence factor. For the Langley 4- by 6-foot vertical tunnel, the turbulence factor is 1.93.)

It is estimated that the angle of attack was set within ±0.1° and that the flap deflection was set within ±0.2°.

Jet-boundary corrections, theoretically determined according to the method given in reference 8, have been applied to the data. No corrections have been made for

the effect of gap between the root section and the tunnel wall or the leakage around the supporting torque tube. The over-all corrections applied (by addition) to the tunnel data are as follows:

$$\Delta\alpha = 2.134C_L \quad \text{(in deg)}$$

$$\Delta C_L = -0.0173C_{L_{tunnel}}$$

$$\Delta C_D = 0.032C_L^2$$

$$\Delta C_m = 0.0072C_L$$

$$\Delta C_{h_f} = kC_L$$

where k is a constant dependent on the chord of the overhang as follows:

c_b/c_f	k
0.09	0.0100
.35	.0078
.50	.0055

DISCUSSION

Lift

Sealing the gap at the flap nose increased the slope of the lift curve C_{L_α}. (See figs. 3 to 12 and table III.) With the gap either sealed or unsealed, the balance nose shape and the amount of overhang appear to have negligible effect upon the values of C_{L_α}.

A summary of the lift effectiveness parameters α_{δ_f} for the various flap configurations is given in table III. The lift effectiveness was greatest for the unsealed flaps with blunt-nose overhangs; however, stall occurred at

lower flap deflections on the blunt nose than on the elliptical nose. With gap sealed, the values of the lift effectiveness parameters were approximately the same for all flaps except for the $0.50c_f$ elliptical-nose overhang, which had a value somewhat smaller. At zero angle of attack, the change of lift with flap deflection for the sealed-gap condition was the same as or slightly greater than for the unsealed-gap condition.

Hinge Moment

The curves of section hinge-moment coefficient were shown in reference 5 to be linear over an approximate range of angle of attack of $\pm 5^{\circ}$ and for flap deflections up to 15°; whereas the curves for the finite-span tail surface (figs. 3 to 12) were, in general, nonlinear.

Flap oscillations (noted on the hinge-moment-coefficient curves by dashed lines) occurred on some balance arrangements as a result of buffeting due to an alternately stalled flow condition. The oscillations increased with flap deflection, overhang, and unsealing the gap. The elliptical-nose flap gave oscillations over a larger range of angle of attack and flap deflection than the blunt-nose flap. Since a flexible torque tube was used in measuring the flap hinge moments, the oscillations depend partly on the torque tube and partly on the mass balance of the flap. Because of the heaviness of the model, the oscillations may be more severe in the wind tunnel than in flight.

The hinge-moment parameters for the various arrangements tested are given in table III. The parameter $C_{h_{f_\alpha}}$ was measured at $\alpha = \delta_f = 0^{\circ}$ and $C_{h_{f_{\delta_f}}}$, between $\delta_f = 0^{\circ}$ and 5°. Although measured at only one point or over a small range, the values of the parameters are useful in comparing some relative merits of the various balance arrangements tested.

Sealing the gap at the flap nose, except on the plain flap, made the value of $C_{h_{f_\alpha}}$ move in a negative direction; sealing the gap made the value of $C_{h_{f_{\delta_f}}}$ move in a negative direction, except on the $0.50c_f$ blunt overhang.

The $0.50c_f$ overhang produced overbalance through a part of the range of flap deflection regardless of the nose shape and gap. (See figs. 9 to 12 and table III.) Overbalance occurred over a wider range of angle of attack and flap deflection in the section data presented in reference 5 than in the finite-span data of the present investigation.

Drag

Although the drag coefficients cannot be considered absolute because of an unknown tunnel correction, the relative values may be independent of tunnel effects. The drag coefficients as functions of angle of attack at various flap deflections are shown in figures 3 to 12. The minimum drag coefficient was obtained with the plain sealed flap and had the value of 0.0110. At large flap deflections for positive angles of attack, the drag coefficients generally increased with increase in overhang and were higher for the blunt nose than for the elliptical nose.

The drag coefficients are plotted in figure 13 against the lift coefficients for the $0.35c_f$ blunt and elliptical overhangs, sealed and unsealed, with $\alpha = 0^\circ$ and δ_f ranging from 0° to 30°. For all these arrangements, the drag coefficients were the same at small lift coefficients and flap deflections. At large flap deflections, the elliptical nose gave more lift than the blunt nose with approximately the same amount of drag.

Pitching Moment

The pitching-moment parameters $\left(C_{m_{C_L}}\right)_{\delta_f}$ and $\left(C_{m_{C_L}}\right)_{\alpha}$ (table III) indicate the position of the aerodynamic center of the airfoil with respect to the $0.35c$ point. When the lift was varied by changing the angle of attack with the flap neutral, the aerodynamic center was located at the $0.22c \pm 0.01c$ station for the various flap arrangements tested. The aerodynamic center of lift due to flap deflection was located at the $0.51c \pm 0.04c$ station, but there was no systematic variation with changes in balance arrangement; the point moved rearward approximately 18 percent with a decrease from infinite aspect ratio to an aspect ratio of 3.

Tab Characteristics

Previous investigations have shown that the tab characteristics of a balanced flap are similar to those for a tab on a plain flap and are generally independent of flap nose shape; hence, only a limited investigation of tab characteristics has been made. This investigation consisted of tests of a balancing tab with $\frac{\partial\delta_t}{\partial\delta_f} = -1$ on the plain sealed flap (fig. 14) and the unsealed $0.35c_f$ elliptical overhang (fig. 15).

The value of $C_{h_{f_{\delta_t}}}$, which shows the effectiveness of the tab in reducing the flap hinge-moment coefficients, was approximately the same for both flaps tested; the value was -0.005 for the sealed plain flap and -0.004 for the unsealed $0.35c_f$ overhang. As was expected, the use of the balancing tab resulted in smaller increments of lift when the flap was deflected. The variation of lift coefficient with tab deflection was approximately the same for both the plain flap and the $0.35c_f$ overhang.

The overbalance of the flap with $0.50c_f$ overhang, which has been previously discussed, could be overcome by the use of a differentially operated unbalancing tab deflected in the same direction as the flap.

Comparison with Data in Two-Dimensional Flow

The lift and hinge-moment parameters of the airfoil and flap were computed from data in two-dimensional flow according to the method of the lifting-line theory presented in reference 5. Edge-velocity corrections to the lifting-line theory for the effect of the chord (reference 6) were applied in the computation of C_{L_α} with the substitution of values for E for the elliptical plan form of the same aspect ratio, where E is the ratio of the semiperimeter to the span. Corrections for streamline curvature for an elliptical plan form were applied to $C_{h_{f_\alpha}}$ (reference 9). These methods of computing C_{L_α} and $C_{h_{f_\alpha}}$ are believed to be the most accurate methods available at the present time.

The lift and hinge-moment parameters, both the measured values and the values computed from section data, are given in table III. The medium-nose overhang referred to in reference 5 had the same nose shape as the elliptical-nose overhang tested in the present investigation. Tunnel corrections, theoretically determined in a manner similar to the method presented in reference 8, were applied to the section hinge-moment coefficients of reference 5 before the parameters were calculated.

The calculated slope of the lift curve generally was slightly higher than the measured slope. The values of the section lift effectiveness parameter α_{δ_f} for the plain flap and for the flap with $0.35c_f$ overhang agreed reasonably well with the finite-span values, but the section values for the flap with $0.50c_f$ overhang were more negative than the finite-span values. Because the flap chord was a constant percentage of the airfoil chord, no corrections were necessary for aspect ratio.

The computed and measured flap hinge-moment parameters are compared in figure 16. The values of $C_{h_{f_\alpha}}$ and $C_{h_{f_{\delta_f}}}$ computed by use of lifting-line theory were more negative than the measured values. Application of additional aspect-ratio corrections, determined from a lifting-surface-theory solution for an elliptical wing (reference 9), made the computed values of $C_{h_{f_\alpha}}$ more positive so as to approach more nearly the measured values of $C_{h_{f_\alpha}}$. Aspect-ratio corrections determined by lifting-surface theory are not yet available for $C_{h_{f_{\delta_f}}}$.

CONCLUSIONS

Tests have been made in three-dimensional flow of an NACA 0009 rectangular semispan tail surface equipped with a plain flap and with balanced flaps of blunt and elliptical nose shapes. The flap chord was 30 percent of the airfoil chord. The results of the present tests and a comparison with previously published results of tests of the same airfoil in two-dimensional flow indicated the following conclusions:

1. Sealing the gap at the flap nose increased the slope of the lift curve, but the balance nose shape and the amount of overhang had little effect on the slope.

2. The effectiveness of the flap $\left(\frac{\partial \alpha}{\partial \delta_f}\right)_{C_L}$ was greatest for the unsealed blunt-nose overhangs, but stall over the flap occurred at lower flap deflections on the blunt-nose than on the elliptical-nose flaps. At zero angle of attack, the variation of lift with flap deflection remained the same or increased with sealing the gap at the flap nose.

3. Sealing the gap at the flap nose made the variation of the flap hinge-moment coefficient with angle of attack or with flap deflection generally move in a negative direction.

4. The 50-percent-flap-chord overhang was overbalanced over a part of the flap deflection range regardless of the nose shape and the gap at the flap nose.

5. When the lift was varied by changing the angle of attack at a flap deflection of 0°, the aerodynamic center was located at approximately the 22-percent-chord station for all arrangements tested. The aerodynamic center of lift due to flap deflection (the aspect ratio being 3) was located at or near the 51-percent-chord station and showed slight but not systematic variation with balance changes.

6. At large flap deflections for positive angles of attack, the drag coefficients generally increased with an increase in overhang and were higher for the blunt nose than for the elliptical nose; at large flap deflections, the elliptical nose gave more lift than the blunt nose with approximately the same amount of drag.

7. The effectiveness of the tab in reducing the flap hinge-moment coefficients was approximately the same for both the sealed plain flap and the unsealed 35-percent-flap-chord elliptical overhang; also, the variation of lift coefficient with tab deflection was approximately the same for both these flap arrangements.

8. The calculation of the finite-span lift and hinge-moment parameters from data in two-dimensional flow

according to the method of lifting-line theory, modified by edge-velocity corrections, showed that the values of the lift-curve slope were slightly higher and the hinge-moment parameters were more negative than the values measured in three-dimensional flow. Application of aspect-ratio corrections determined from a lifting-surface-theory solution for an elliptical plan form made the computed values of the variation of the hinge-moment coefficient with angle of attack more positive so as to approach more nearly the measured values.

Langley Memorial Aeronautical Laboratory
National Advisory Committee for Aeronautics
Langley Field, Va.,

REFERENCES

1. Sears, Richard I.: Wind-Tunnel Investigation of Control-Surface Characteristics. I - Effect of Gap on the Aerodynamic Characteristics of an NACA 0009 Airfoil with a 30-Percent-Chord Plain Flap. NACA ARR, June 1941.

2. Sears, Richard I., and Hoggard, H. Page, Jr.: Wind-Tunnel Investigation of Control-Surface Characteristics. II - A Large Aerodynamic Balance of Various Nose Shapes with a 30-Percent-Chord Flap on an NACA 0009 Airfoil. NACA ARR, Aug. 1941.

3. Ames, Milton B., Jr.: Wind-Tunnel Investigation of Control-Surface Characteristics. III - A Small Aerodynamic Balance of Various Nose Shapes Used with a 30-Percent-Chord Flap on an NACA 0009 Airfoil. NACA ARR, Aug. 1941.

4. Ames, Milton B., Jr., and Eastman, Donald R., Jr.: Wind-Tunnel Investigation of Control-Surface Characteristics. IV - A Medium Aerodynamic Balance of Various Nose Shapes Used with a 30-Percent-Chord Flap on an NACA 0009 Airfoil. NACA ARR, Sept. 1941.

5. Sears, Richard I.: Wind-Tunnel Data on the Aerodynamic Characteristics of Airplane Control Surfaces. NACA ACR No. 3L08, 1943.

6. Jones, Robert T.: Correction of the Lifting-Line Theory for the Effect of the Chord. NACA TN No. 817, 1941.

7. Wenzinger, Carl J., and Harris, Thomas A.: The Vertical Wind Tunnel of the National Advisory Committee for Aeronautics. NACA Rep. No. 387, 1931.

8. Swanson, Robert S., and Toll, Thomas A.: Jet-Boundary Corrections for Reflection-Plane Models in Rectangular Wind Tunnels. NACA ARR No. 3E22, 1943.

9. Swanson, Robert S., and Gillis, Clarence L.: Limitations of Lifting-Line Theory for Estimation of Aileron Hinge-Moment Characteristics. NACA CB No. 3L02, 1943.

TABLE I

ORDINATES FOR NACA 0009 AIRFOIL

(All dimensions in percent chord)

Station	Ordinates	
	Upper	Lower
0	0	0
1.25	1.42	-1.42
2.5	1.96	-1.96
5.0	2.67	-2.67
7.5	3.15	-3.15
10	3.51	-3.51
15	4.01	-4.01
20	4.30	-4.30
25	4.46	-4.46
30	4.50	-4.50
40	4.35	-4.35
50	3.97	-3.97
60	3.42	-3.42
70	2.75	-2.75
80	1.97	-1.97
90	1.09	-1.09
95	.60	-.60
100	(.10)	(-.10)
100	0	0
L.E. radius = 0.89		

NATIONAL ADVISORY
COMMITTEE FOR AERONAUTICS

TABLE II

ELLIPTICAL-OVERHANG PROFILE

(All dimensions in percent chord)

$0.35c_f$ overhang		$0.50c_f$ overhang	
Station	Ordinate	Station	Ordinate
0	0	0	0
.15	.54	.35	.88
.50	.97	.85	1.26
1.00	1.33	1.85	1.68
2.00	1.79	2.85	1.96
3.00	2.09	3.85	2.15
4.00	2.30	4.85	2.30
5.00	2.45	5.85	2.42
7.00	2.64	6.85	2.52
9.00	2.71	8.85	2.64
		10.85	2.70
		12.85	2.72
L.E. radius = 1.05		L.E. radius = 1.23	

NATIONAL ADVISORY
COMMITTEE FOR AERONAUTICS

TABLE III

PARAMETER VALUES FOR A 0.30c FLAP ON A RECTANGULAR SEMISPAN TAIL SURFACE

NATIONAL ADVISORY COMMITTEE FOR AERONAUTICS

$\frac{c_b}{c_f}$	$\frac{\delta_t}{\delta_f}$	Gap	Balance nose shape	$\left(\frac{\partial C_L}{\partial \alpha}\right)_{\delta_f}$		$\left(\frac{\partial \alpha}{\partial \delta_f}\right)_{C_L}$		$\left(\frac{\partial C_{h_f}}{\partial \alpha}\right)_{\delta_f}$			$\left(\frac{\partial C_{h_f}}{\partial \delta_f}\right)_{\alpha}$		$\left(\frac{\partial C_m}{\partial C_L}\right)_{\delta_f}$	$\left(\frac{\partial C_m}{\partial C_L}\right)_{\alpha}$
				Measured value	Value computed from section data (a)	Measured value	Value obtained from section data	Measured value	Value computed from section data (a)	Value computed from section data (b)	Measured value	Value computed from section data (a)	Measured value (c)	Measured value (c)
----	0	Sealed	Plain	0.055	0.057	-0.64	-0.58	-0.0020	-0.0034	-0.0016	-0.0082	-0.0098	0.118	-0.147
----	-1	Sealed	Plain	.055	--------	-.50	--------	-.0020	--------	--------	-.0029	--------	.118	-.125
----	0	0.005c	Plain	.054	.055	-.60	-.60	-.0024	-.0034	-.0017	-.0080	-.0104	.118	-.127
0.35	0	Sealed	Blunt	.054	.055	-.64	-.64	-.0005	-.0016	-.0003	-.0028	-.0029	.126	-.170
.35	0	0.005c	Blunt	.050	.051	-.67	-.68	.0009	-.0014	-.0002	-.0025	-.0029	.120	-.147
.35	0	Sealed	Elliptical	.055	.055	-.62	-.60	-.0010	-.0019	-.0006	-.0060	-.0064	.118	-.139
.35	0	0.005c	Elliptical	.050	.052	-.58	-.55	0	-.0017	-.0004	-.0052	-.0055	.130	-.200
.35	-1	0.005c	Elliptical	.051	--------	-.46	--------	-.0010	--------	--------	-.0007	--------	.127	-.182
.50	0	Sealed	Blunt	.054	.056	-.64	-.72	.0025	.0001	.0011	.0064	.0023	.126	-.141
.50	0	0.005c	Blunt	.050	[d].048	-.65	[d]-.73	.0036	[e].0012	[e].0020	.0060	[e].0040	.120	-.120
.50	0	Sealed	Elliptical	.054	.056	-.58	-.70	-.0003	-.0004	.0006	-.0024	-.0043	.139	-.172
.50	0	0.005c	Elliptical	.052	[d].051	-.59	[d]-.61	.0009	[e].0003	[e].0012	-.0004	[e]-.0032	.121	-.171

[a]Computed from section data with edge-velocity corrections (reference 6).

[b]Computed from section data with edge-velocity corrections (reference 6) and streamline-curvature corrections (reference 9).

[c]Measured about 0.35c point.

[d]Computed values represent extrapolations from test points from reference 5.

[e]Gap, 0.001c.

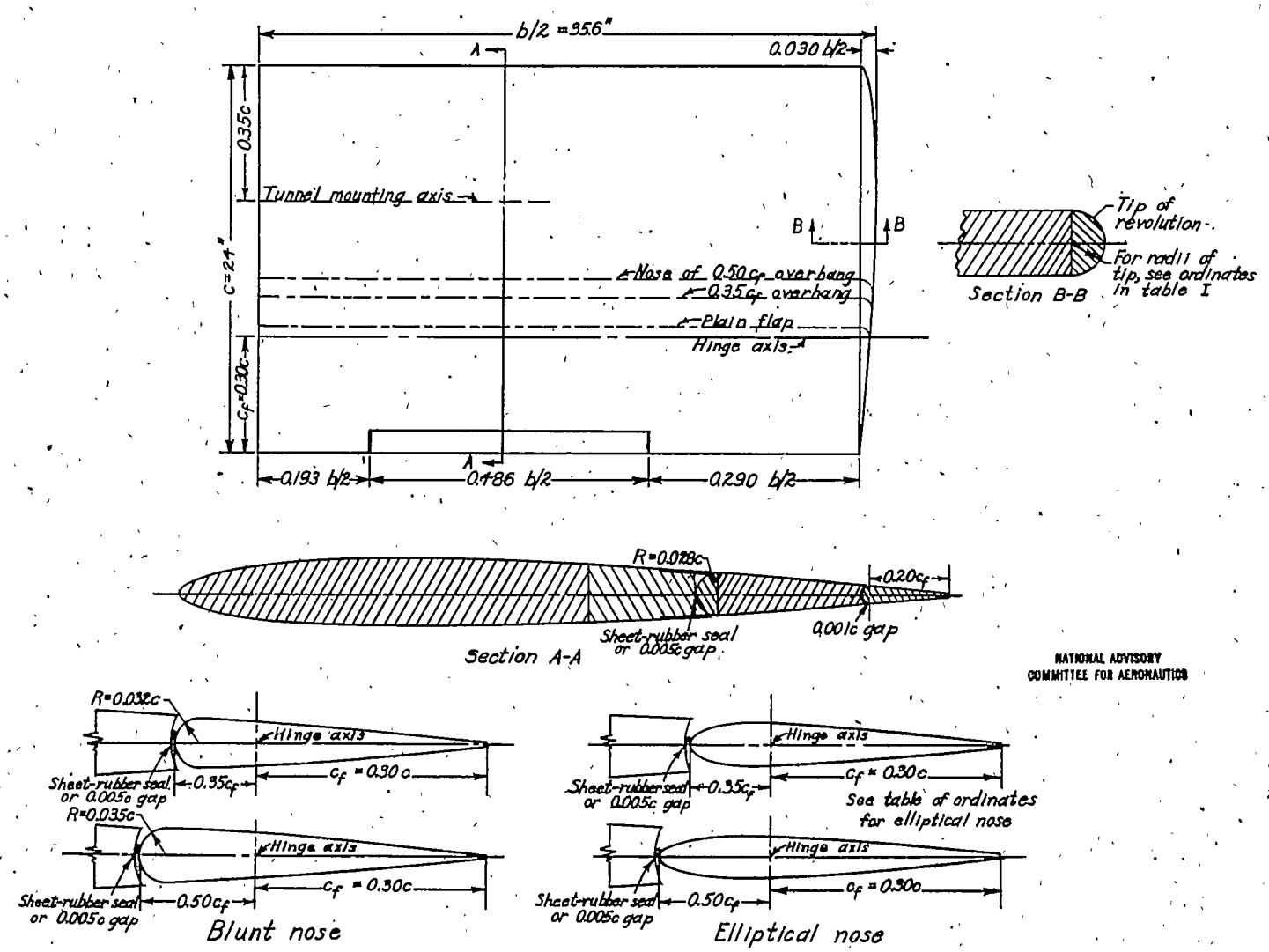

NATIONAL ADVISORY COMMITTEE FOR AERONAUTICS

Figure 1.- Details of an NACA 0009 rectangular semispan tail surface. Aspect ratio = 3.

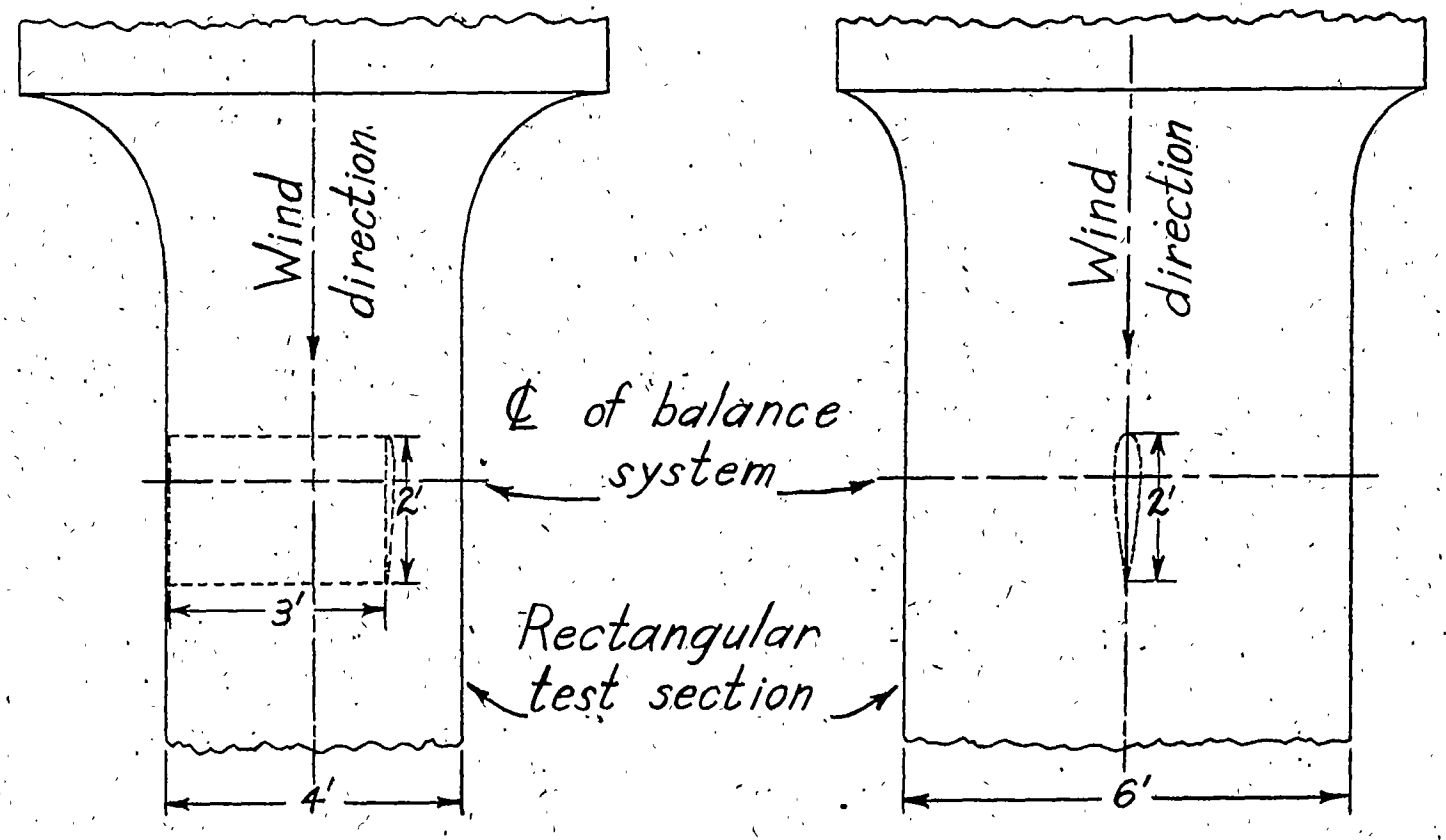

NATIONAL ADVISORY COMMITTEE FOR AERONAUTICS

Figure 2.-Semispan model mounted in the Langley 4-by 6-foot vertical tunnel.

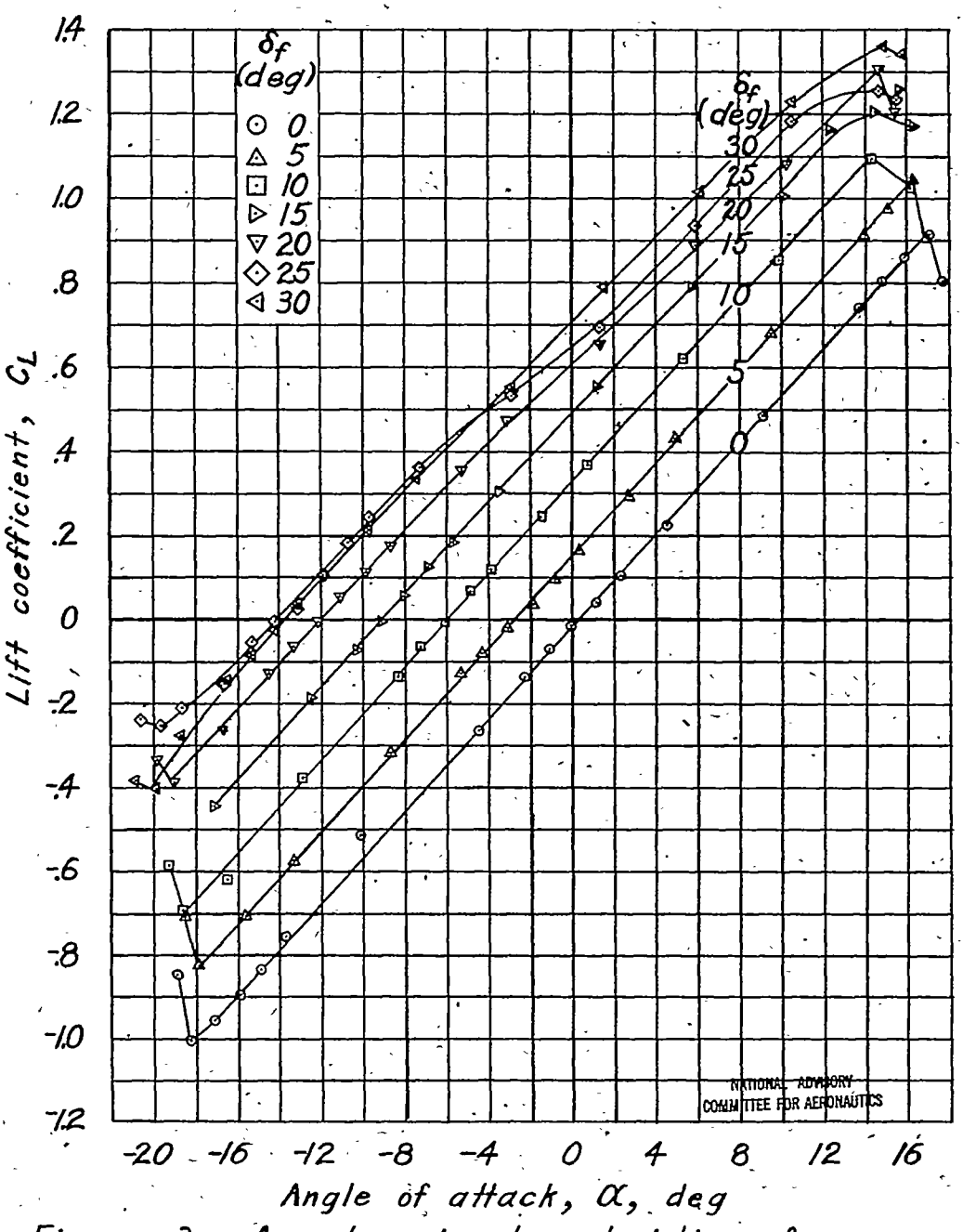

Figure 3.- Aerodynamic characteristics of a rectangular semispan tail surface. Plain flap; sealed gap; $\delta_t = 0^\circ$; 0.30c flap; A=3.

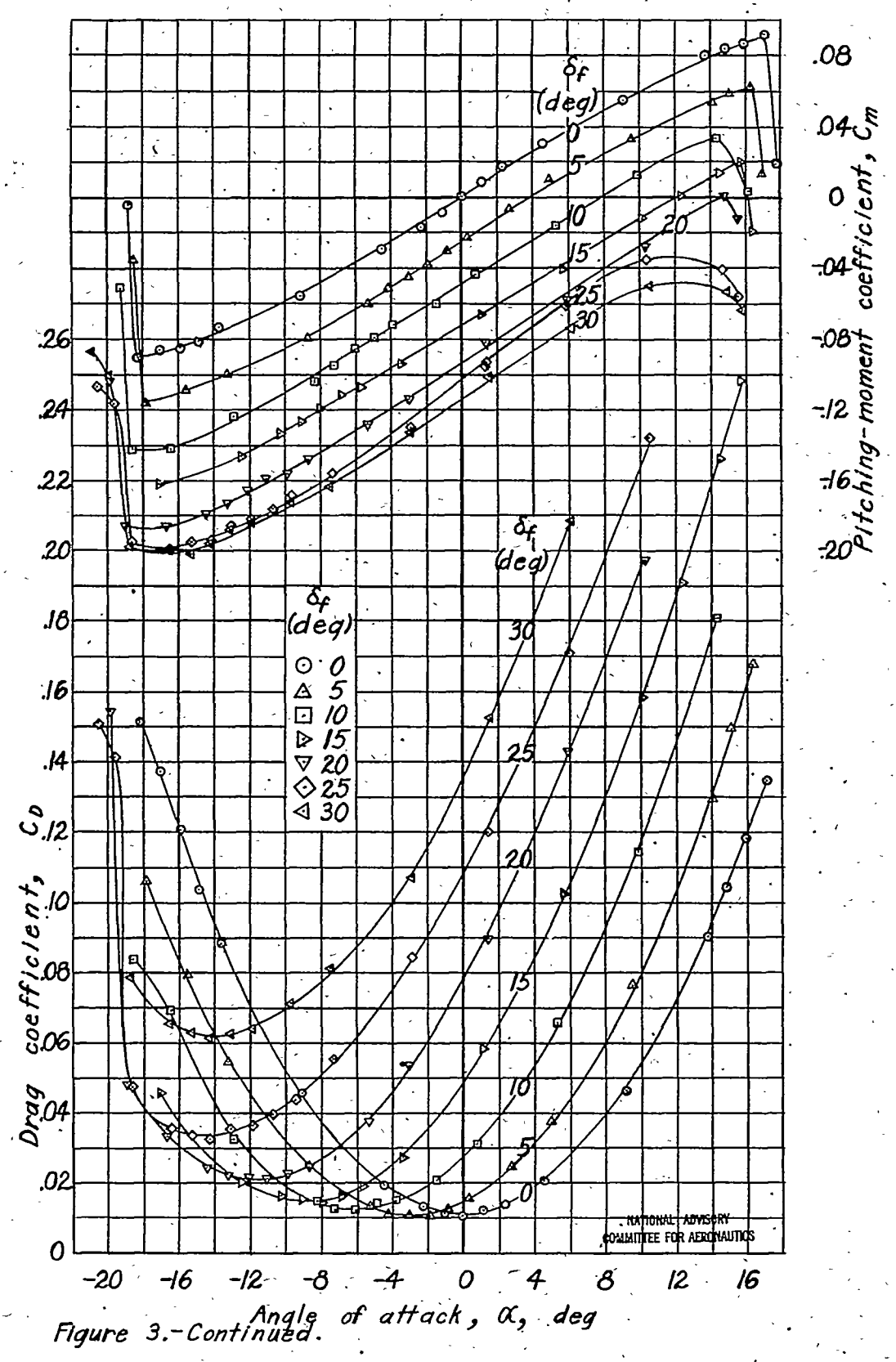

Figure 3.-Continued.

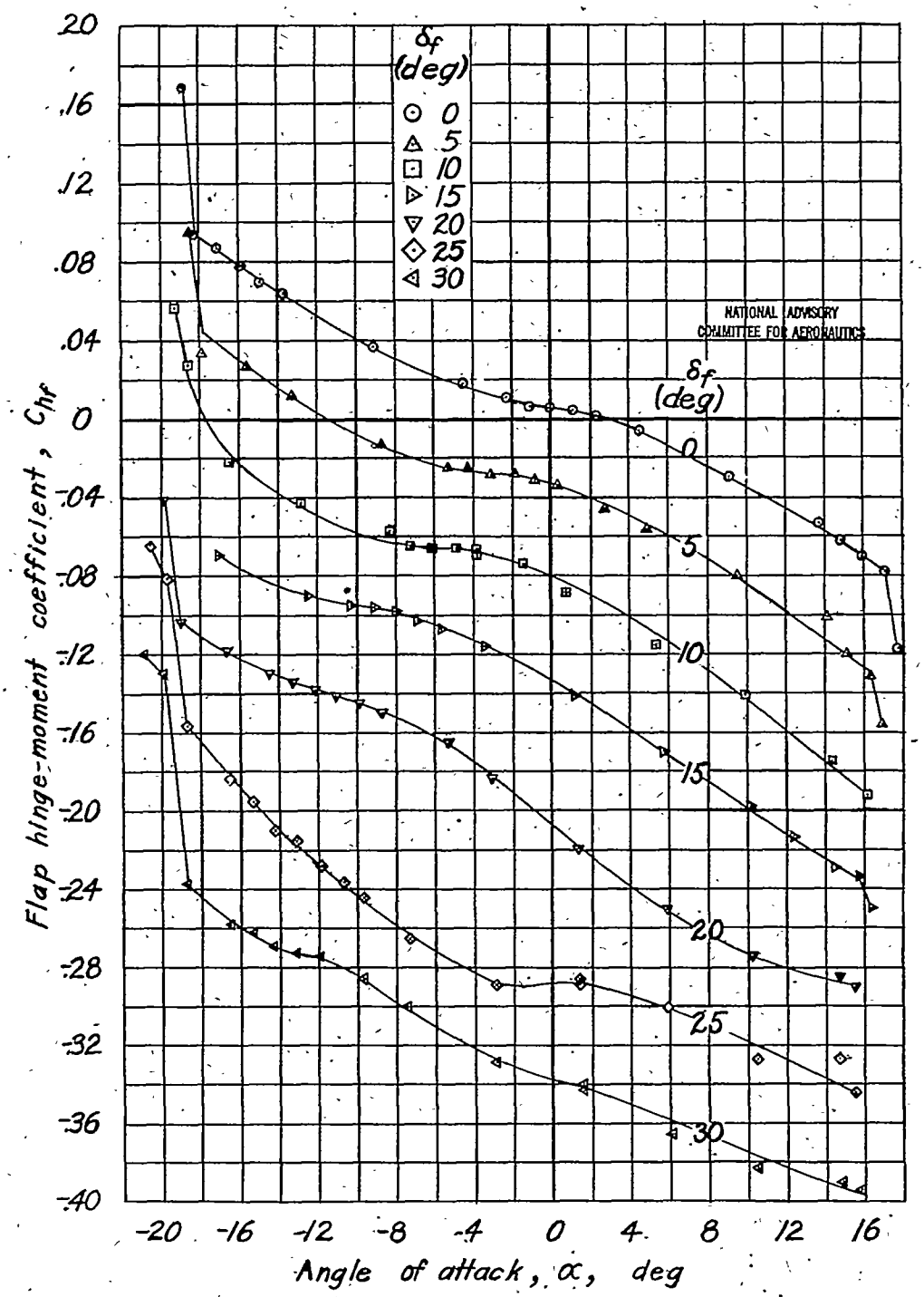

Figure 3.- Concluded.

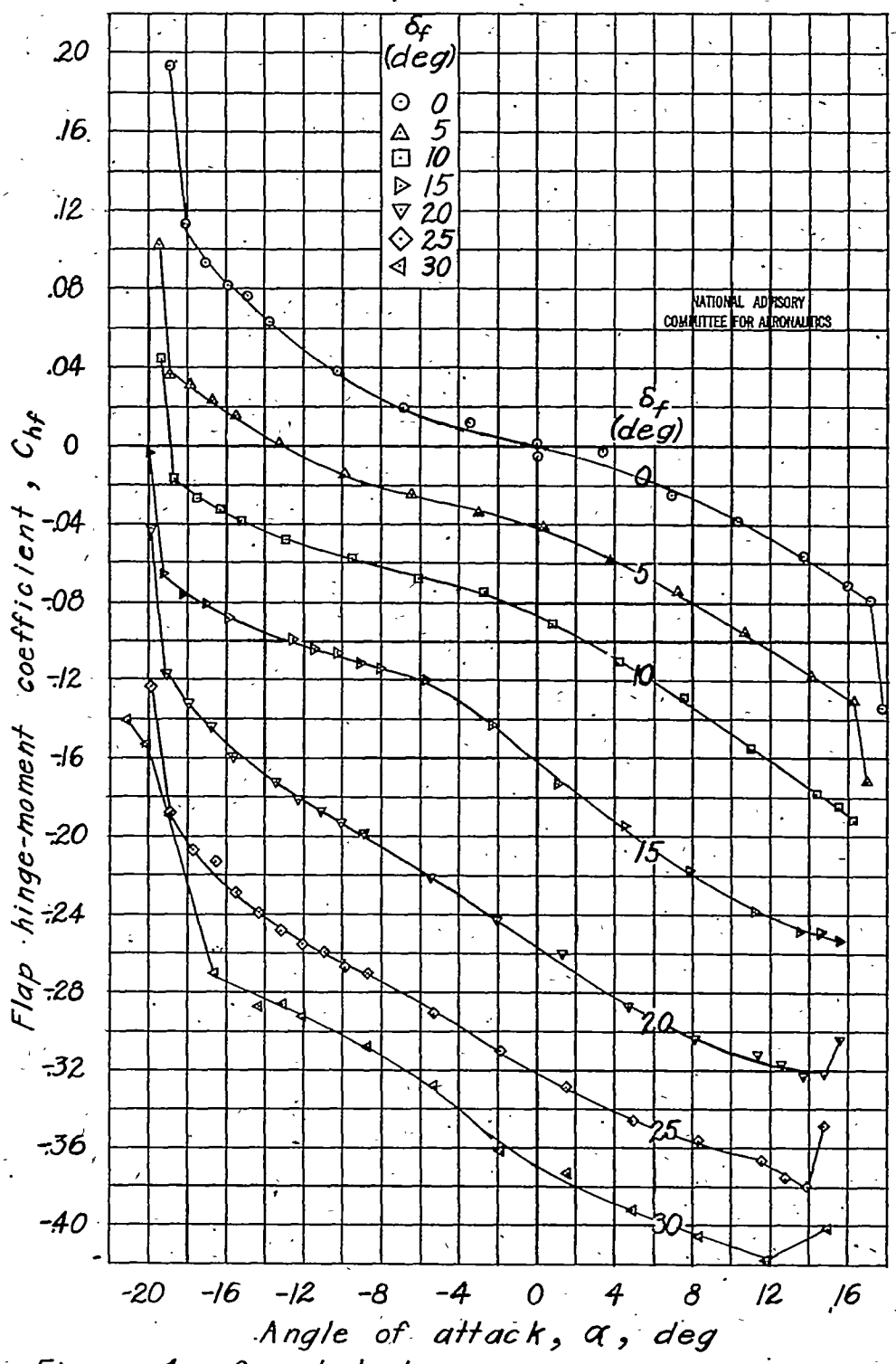

Figure 4.- Concluded.

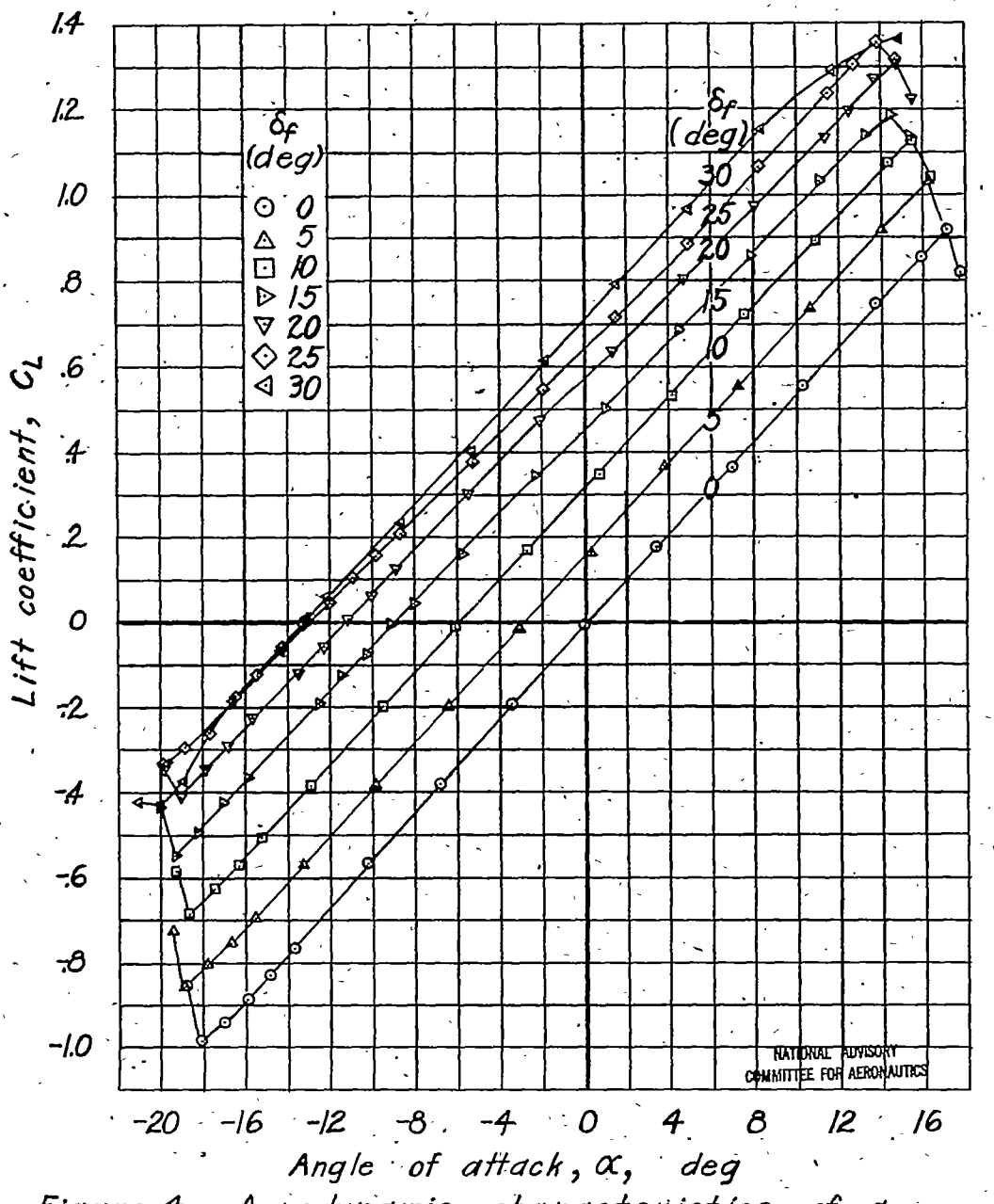

Figure 4.- Aerodynamic characteristics of a rectangular semispan tail surface. Plain flap; 0.005c gap; $\delta_t = 0^\circ$; 0.30c flap; A = 3.

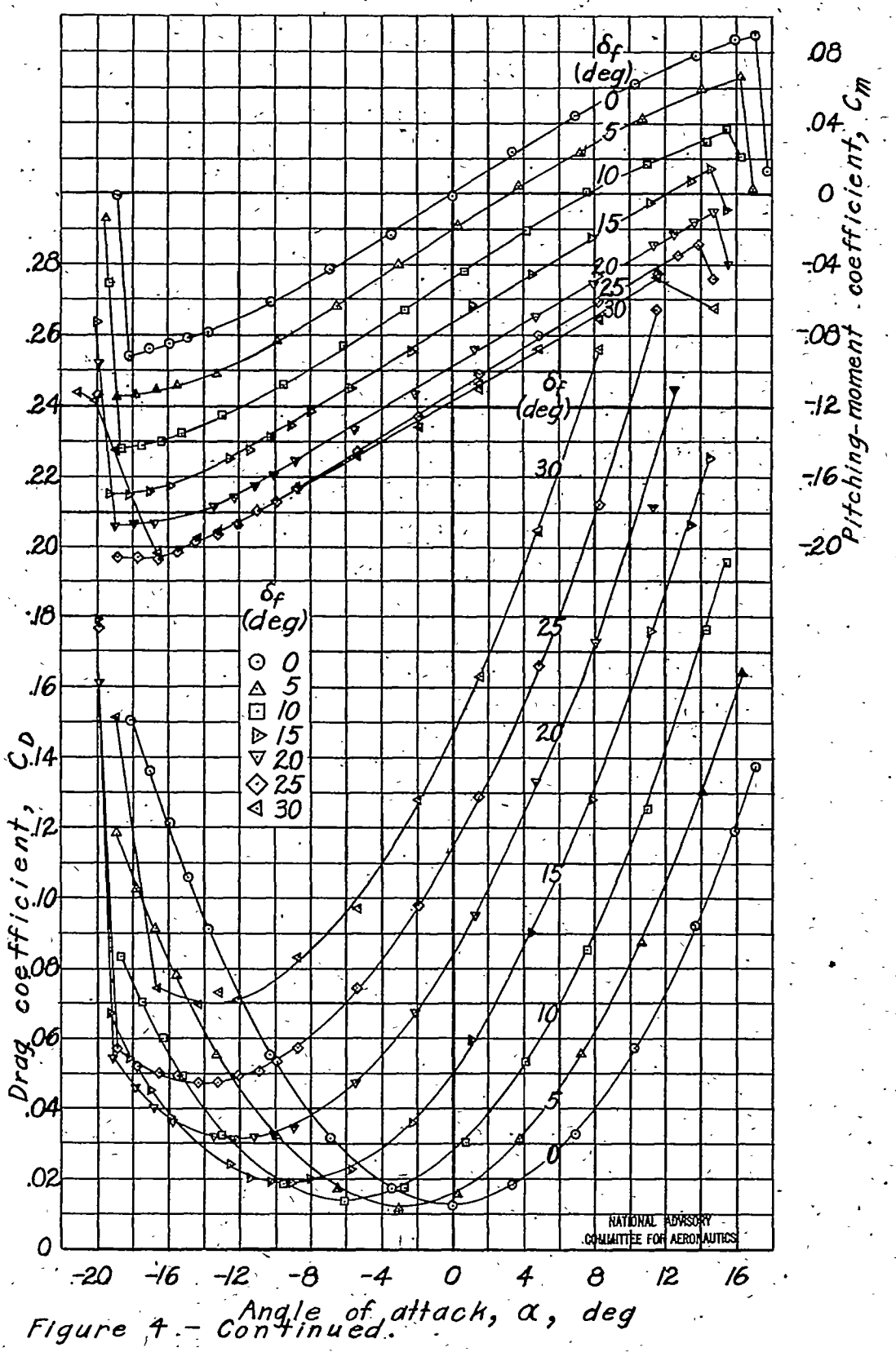

Figure 4.- Continued.

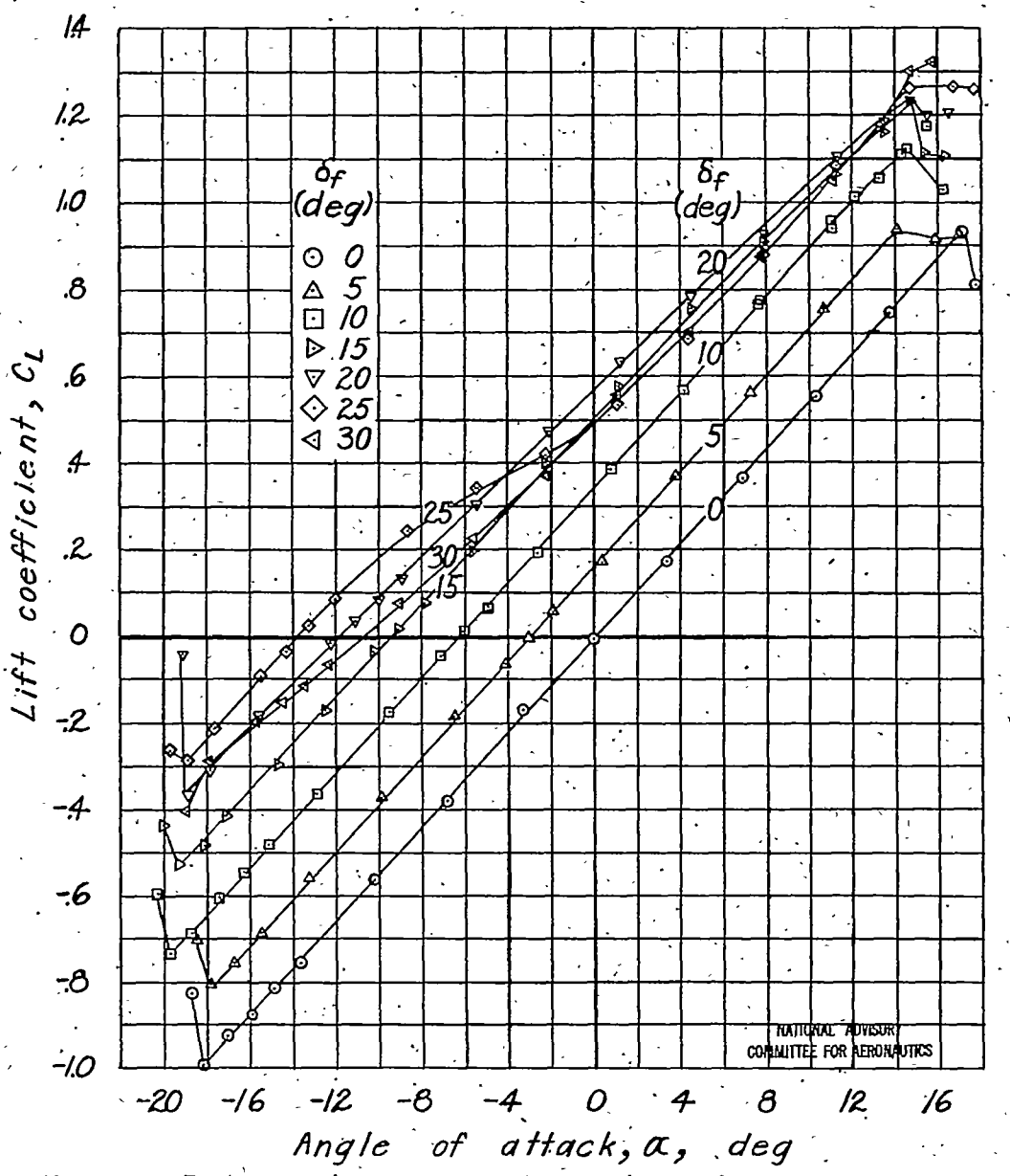

Figure 5.- Aerodynamic characteristics of a rectangular semispan tail surface. Flap with $0.35c_f$ blunt overhang; sealed gap; $\delta_t = 0^\circ$; 0.30c flap; A=3.

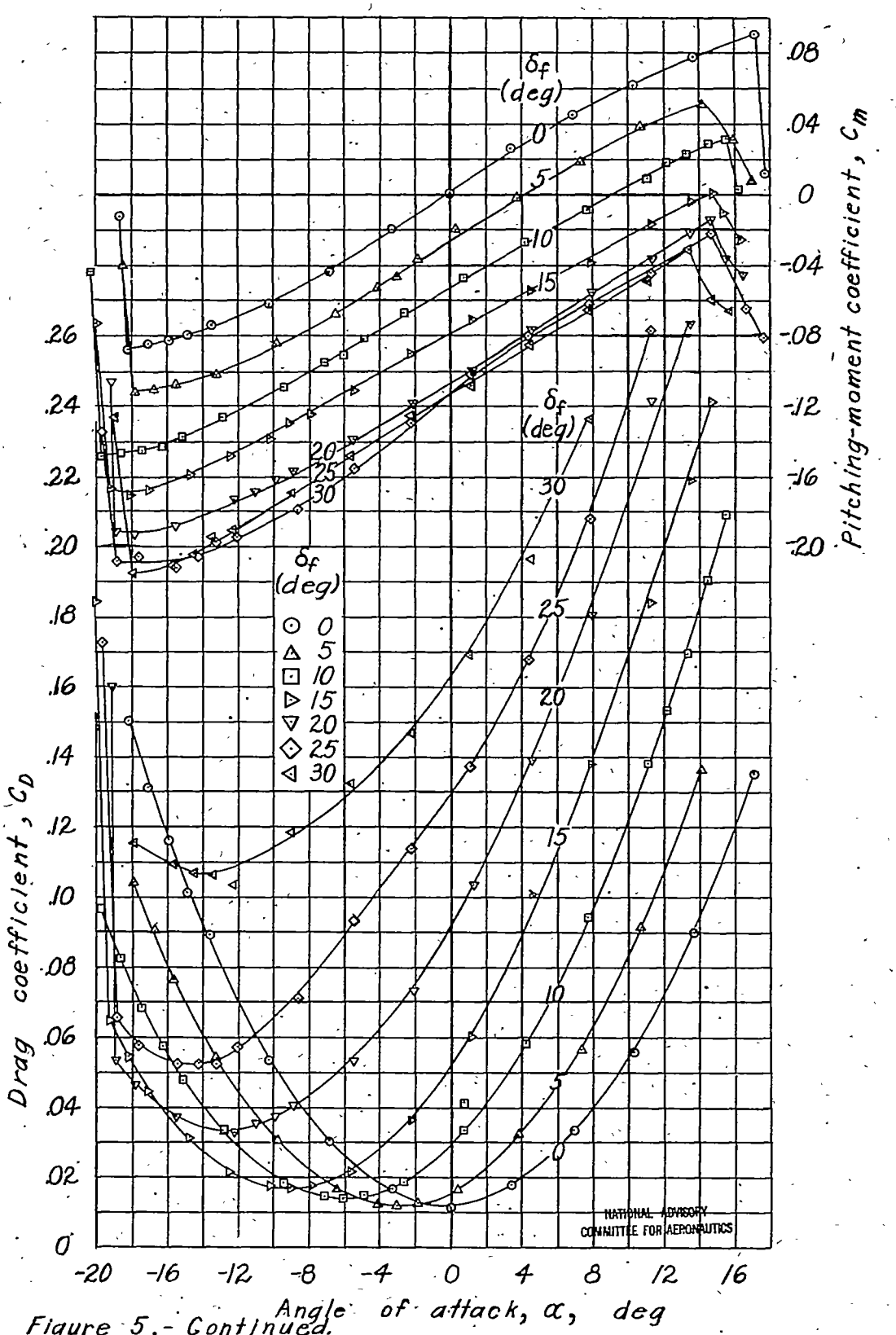

Figure 5.- Continued.

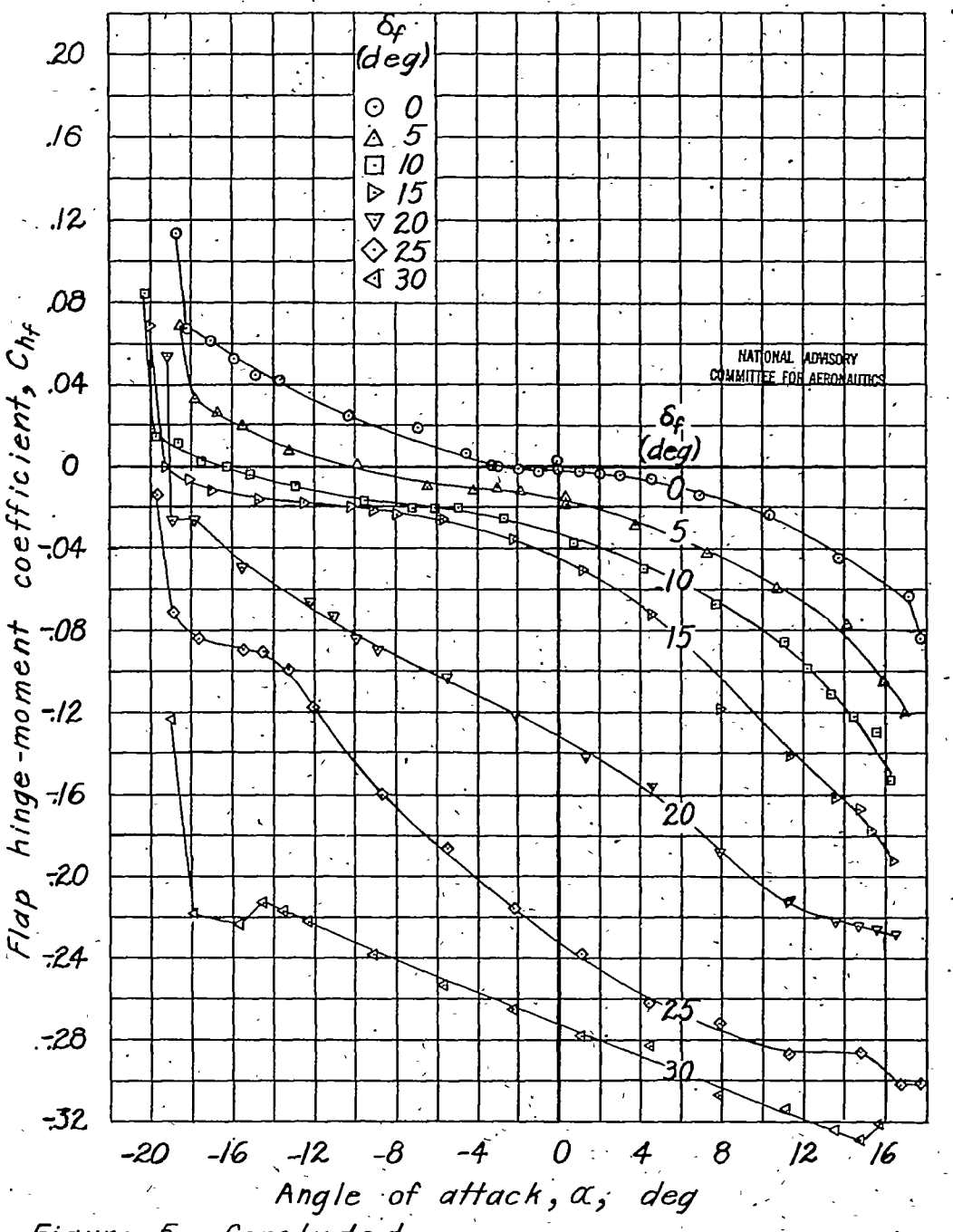

Figure 5.- Concluded.

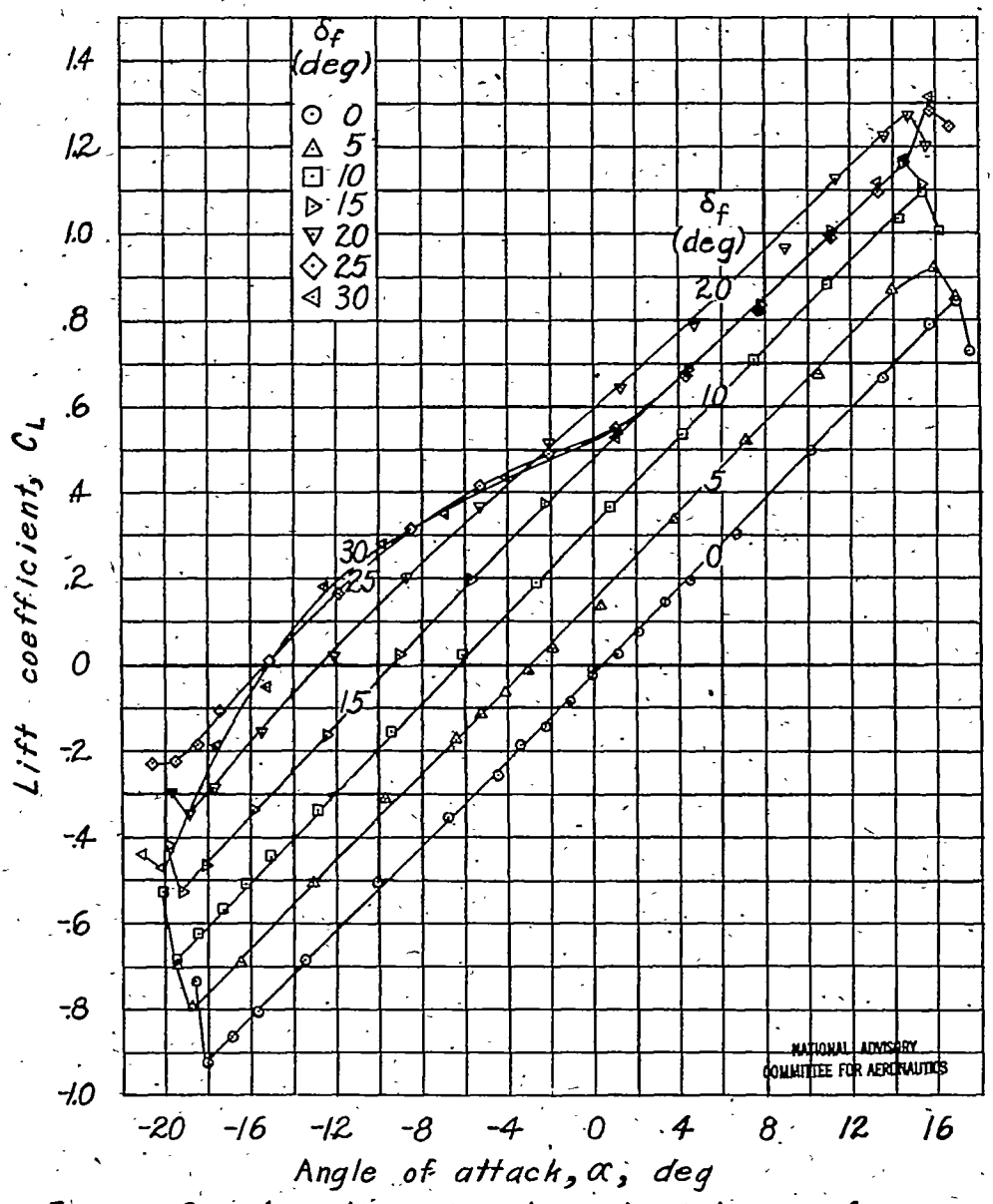

Figure 6.- Aerodynamic characteristics of a rectangular semispan tail surface. Flap with 0.35 c_f blunt overhang; 0.005 c gap; $\delta_t = 0°$; 0.30c flap; A = 3.

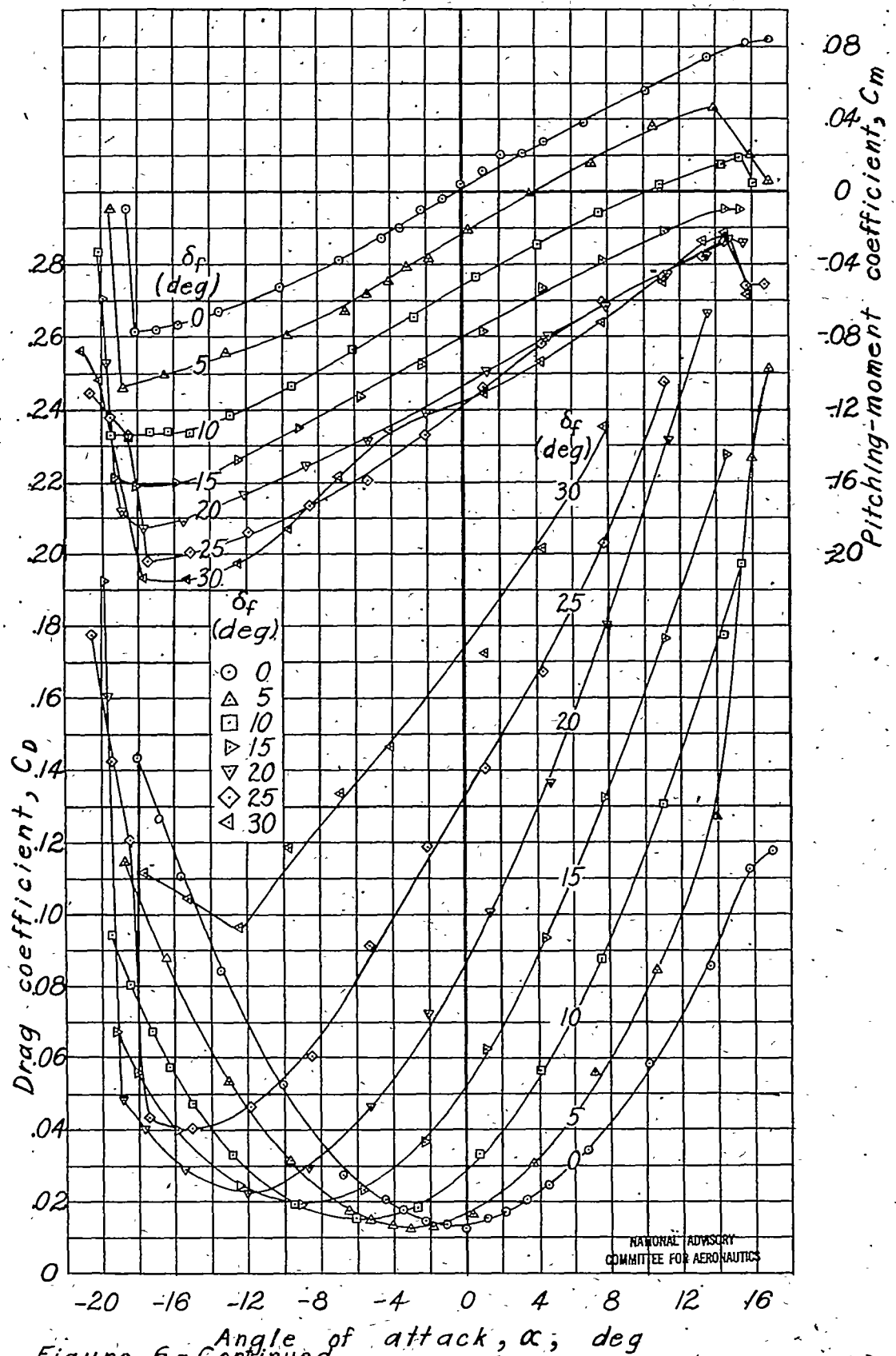

Figure 6.- Continued.

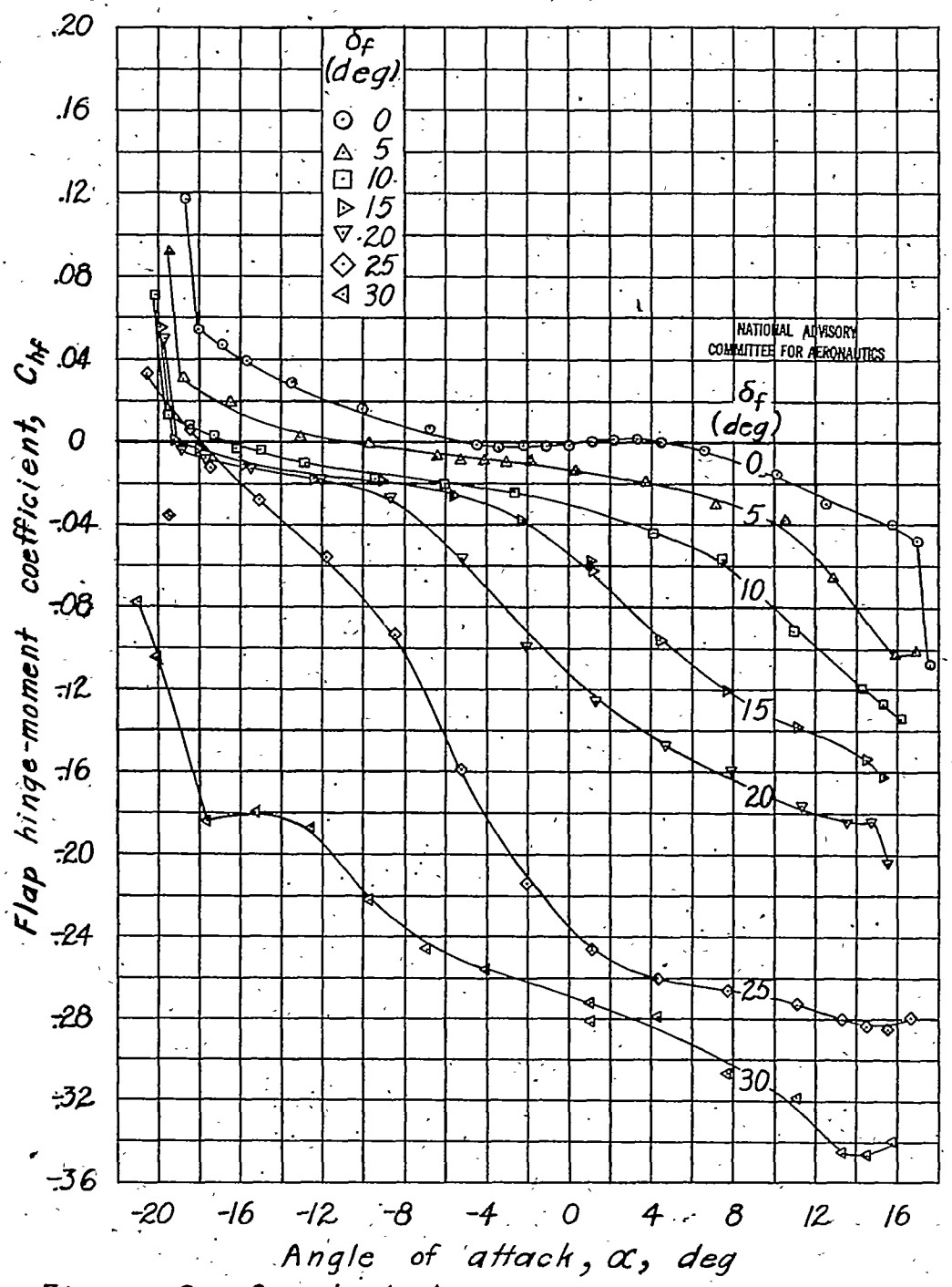

Figure 6.- Concluded.

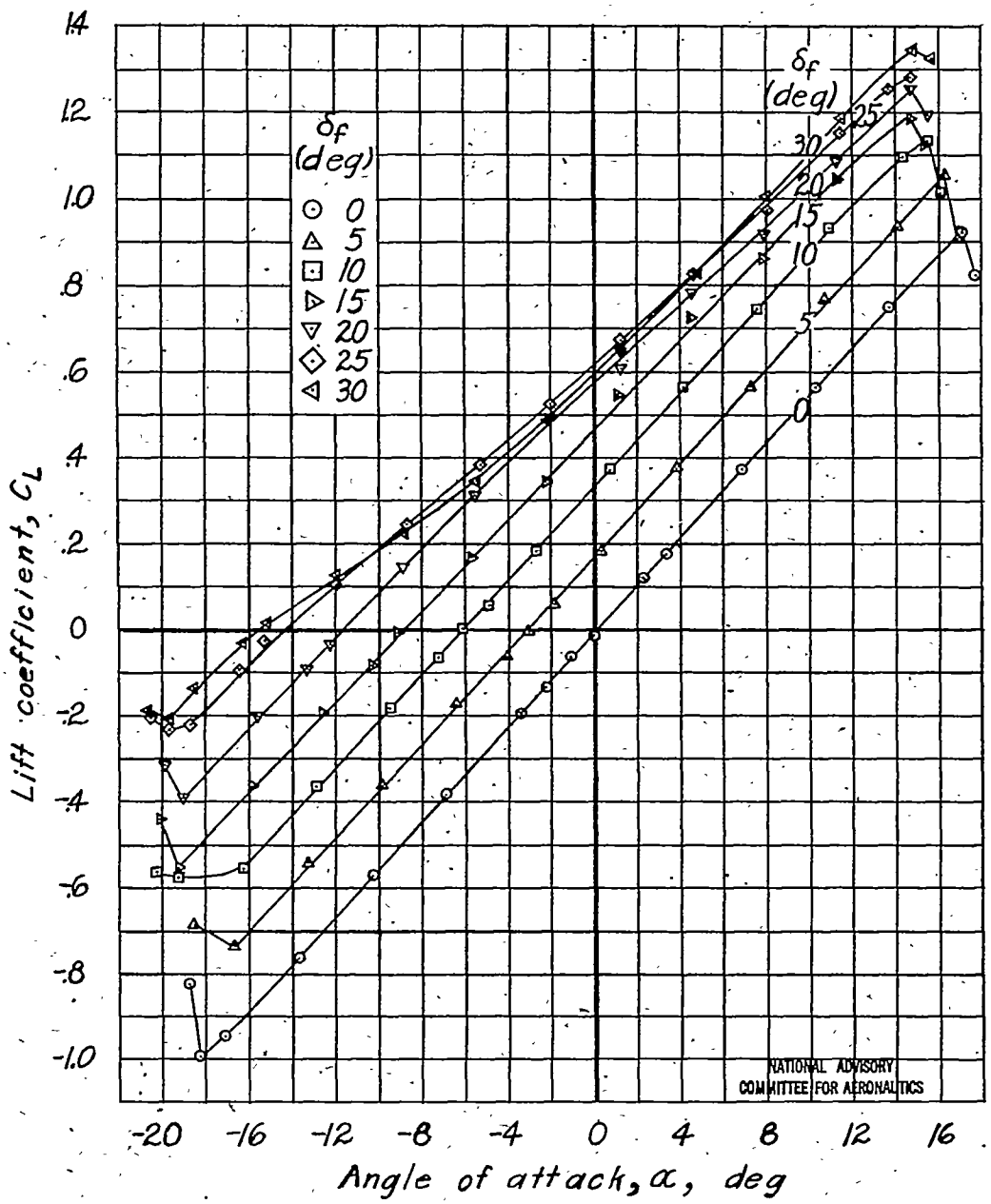

Figure 7.- Aerodynamic characteristics of a rectangular semispan tail surface. Flap with $0.35c_f$ elliptical overhang; sealed gap; $\delta_t = 0^\circ$; $0.30c$ flap; $A = 3$.

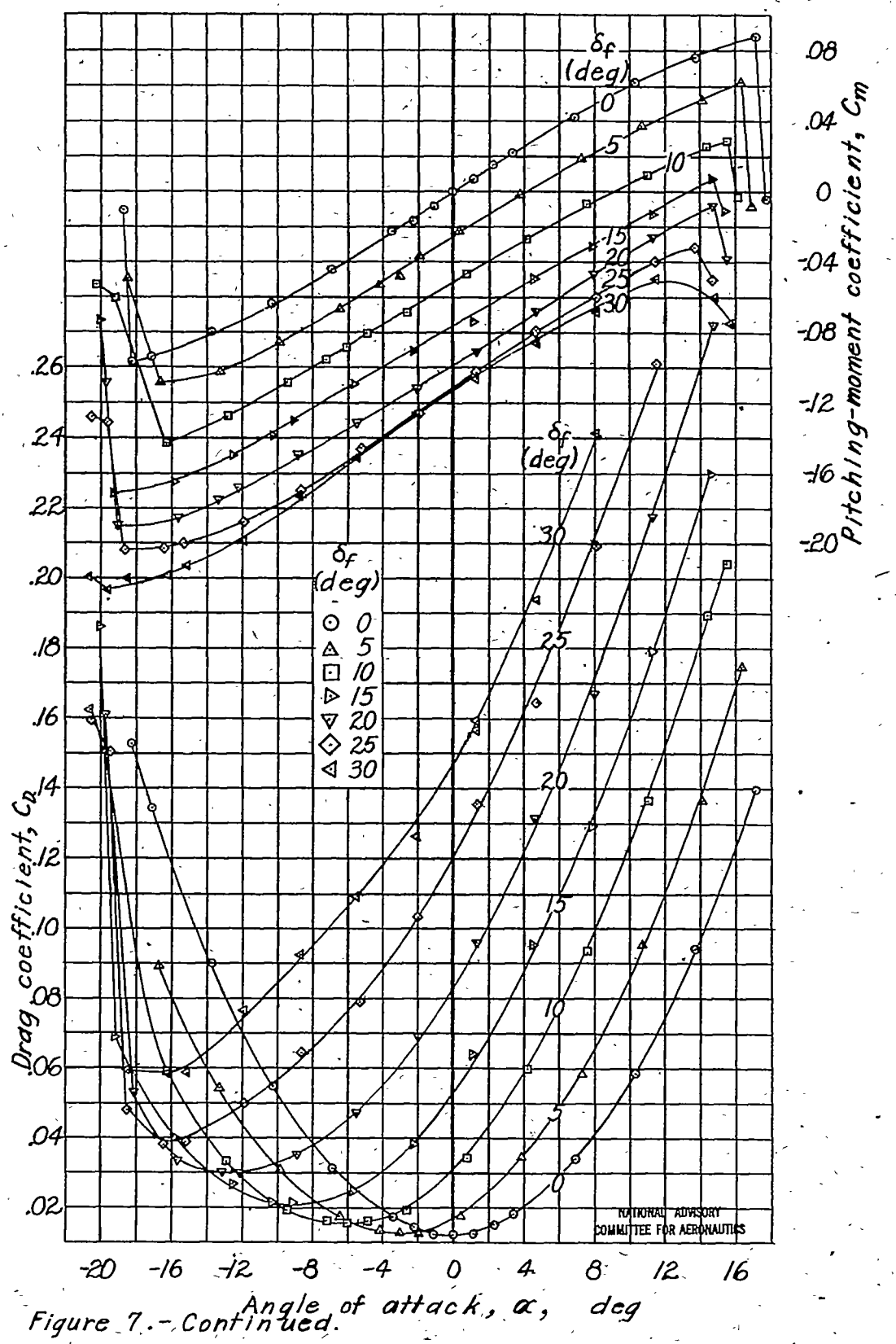

Figure 7.- Continued.

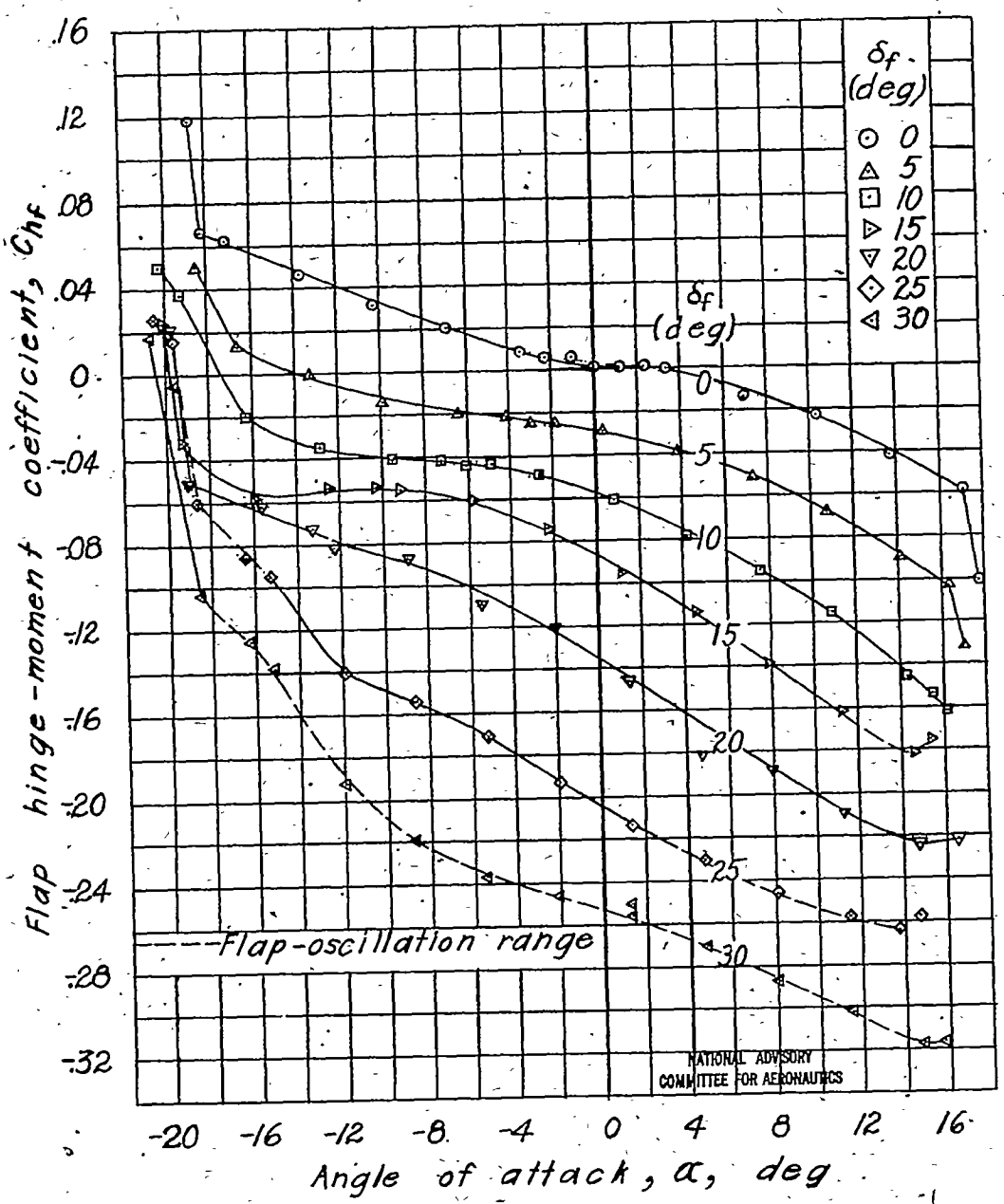

Figure 7.- Concluded.

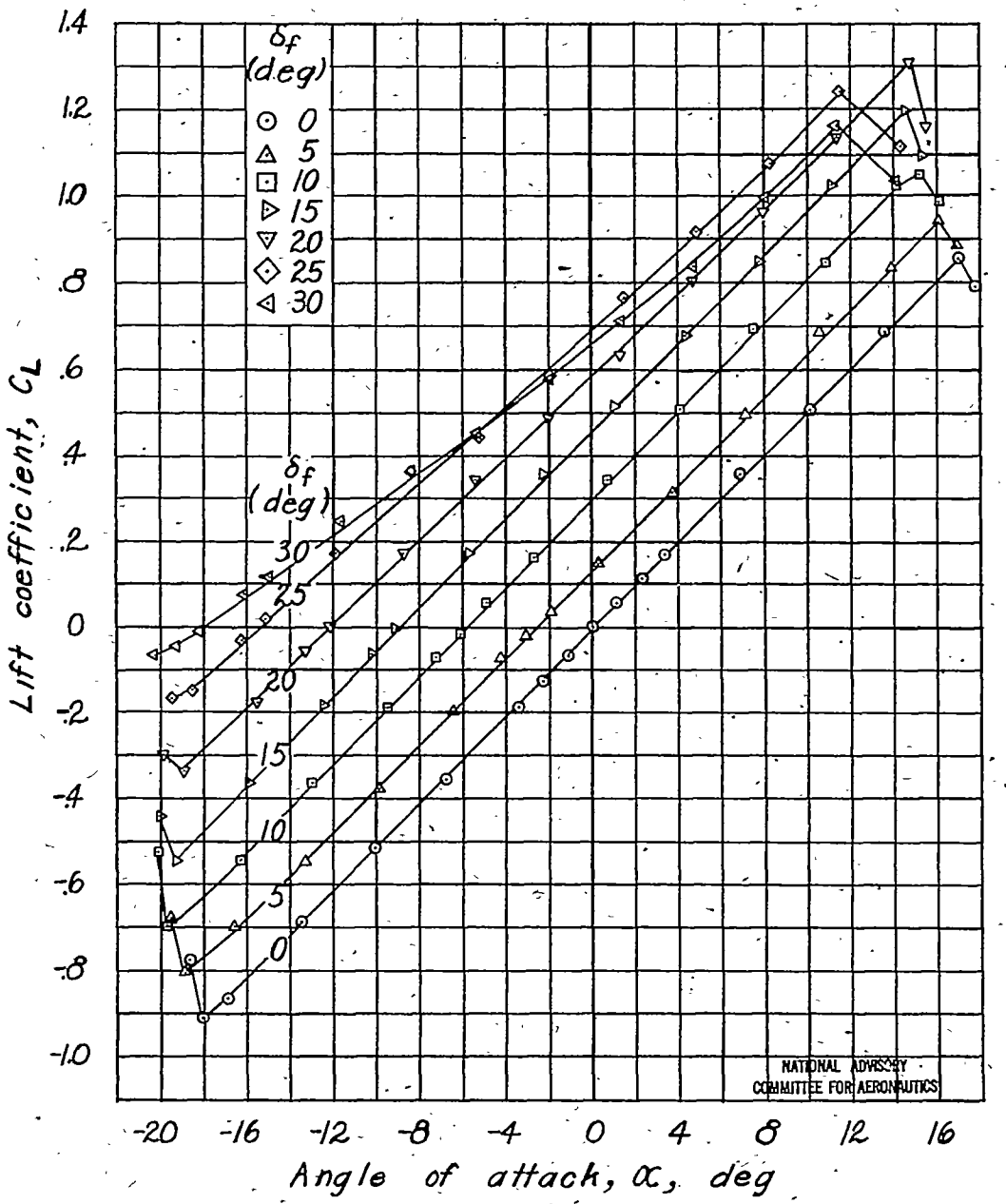

Figure 8.- Aerodynamic characteristics of a rectangular semispan tail surface. Flap with 0.35 c_f elliptical overhang; 0.005c gap; $\delta_t = 0°$; 0.30c flap; A=3.

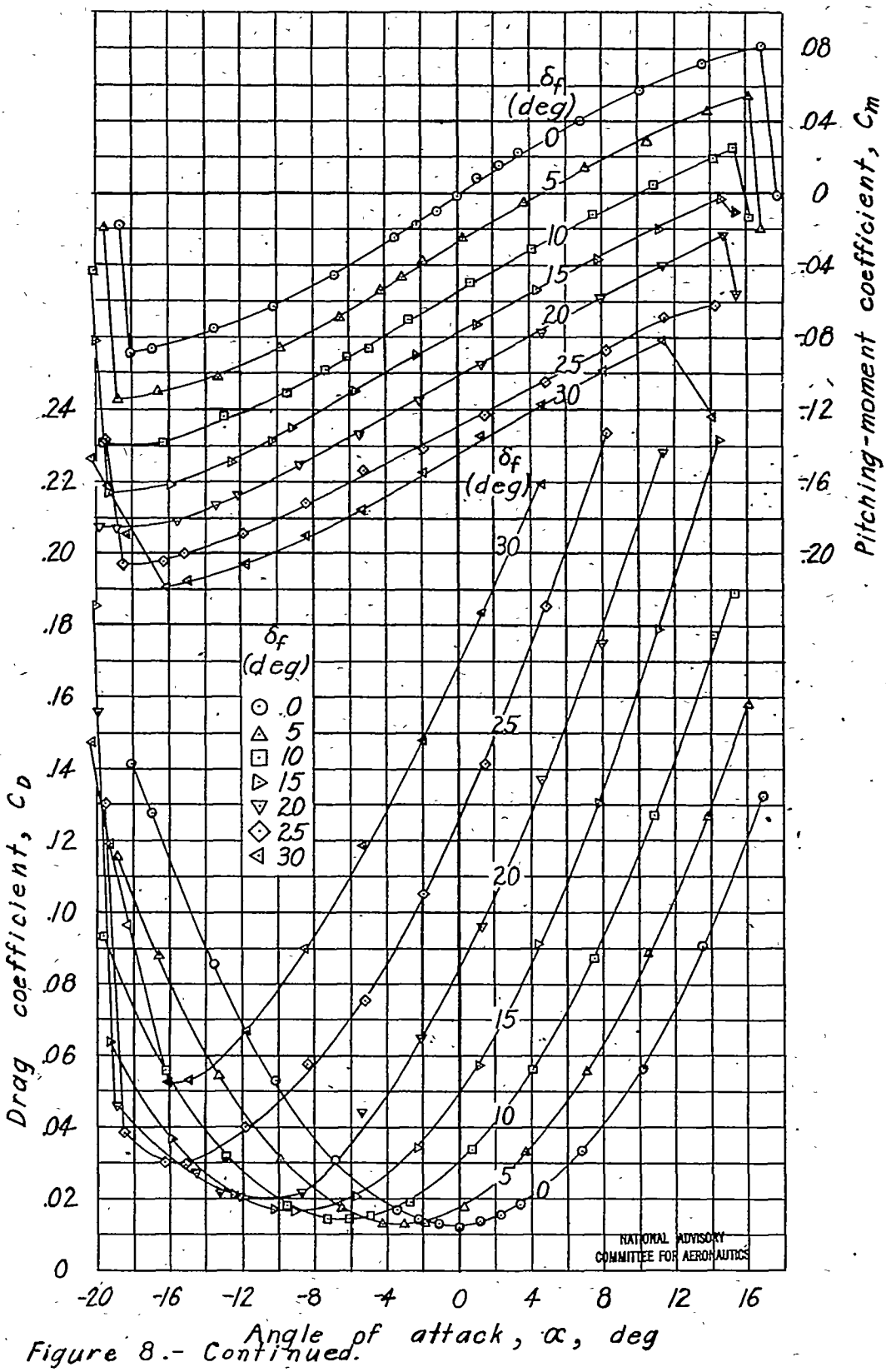

Figure 8.- Continued.

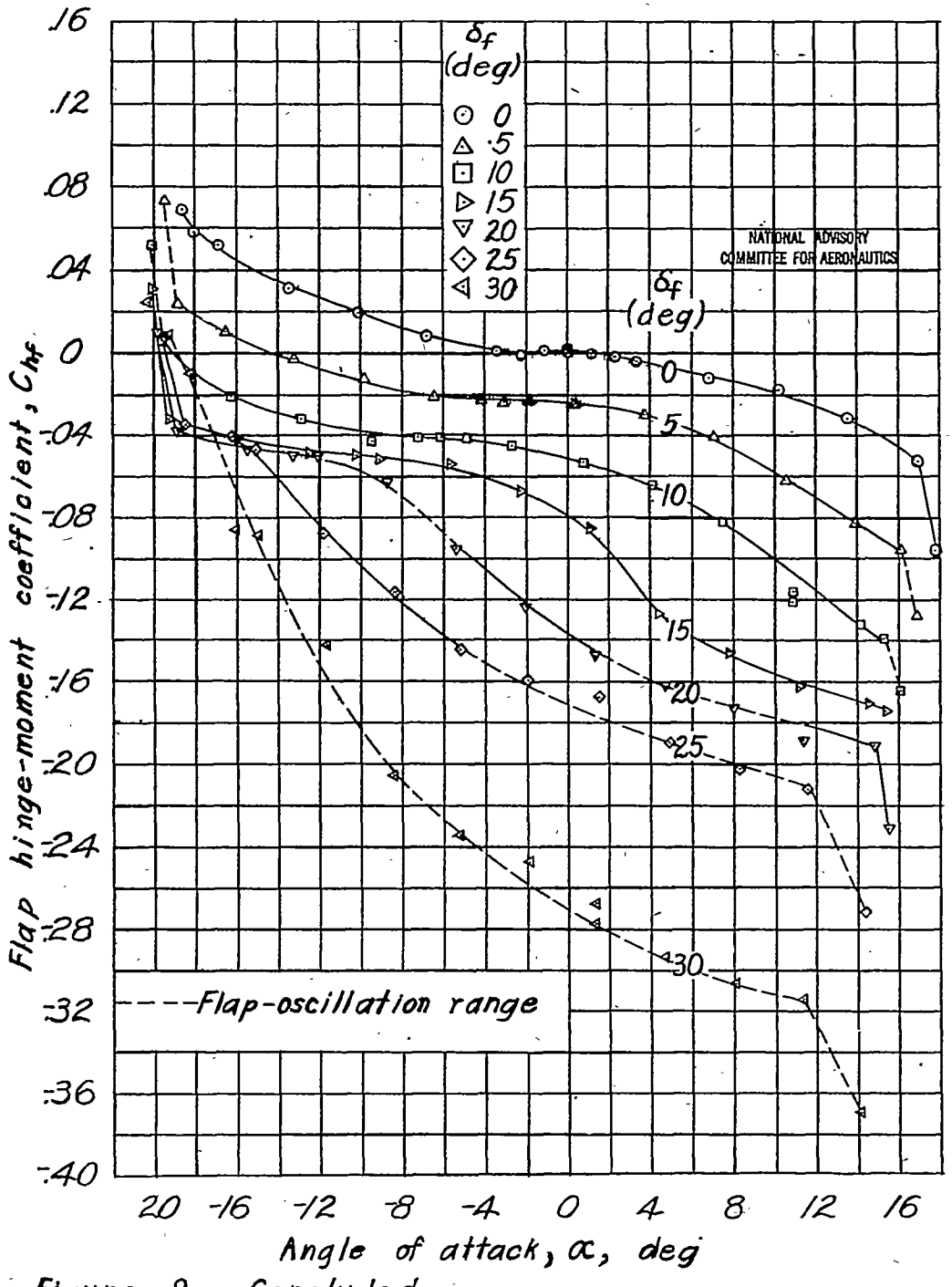

Figure 8.- Concluded.

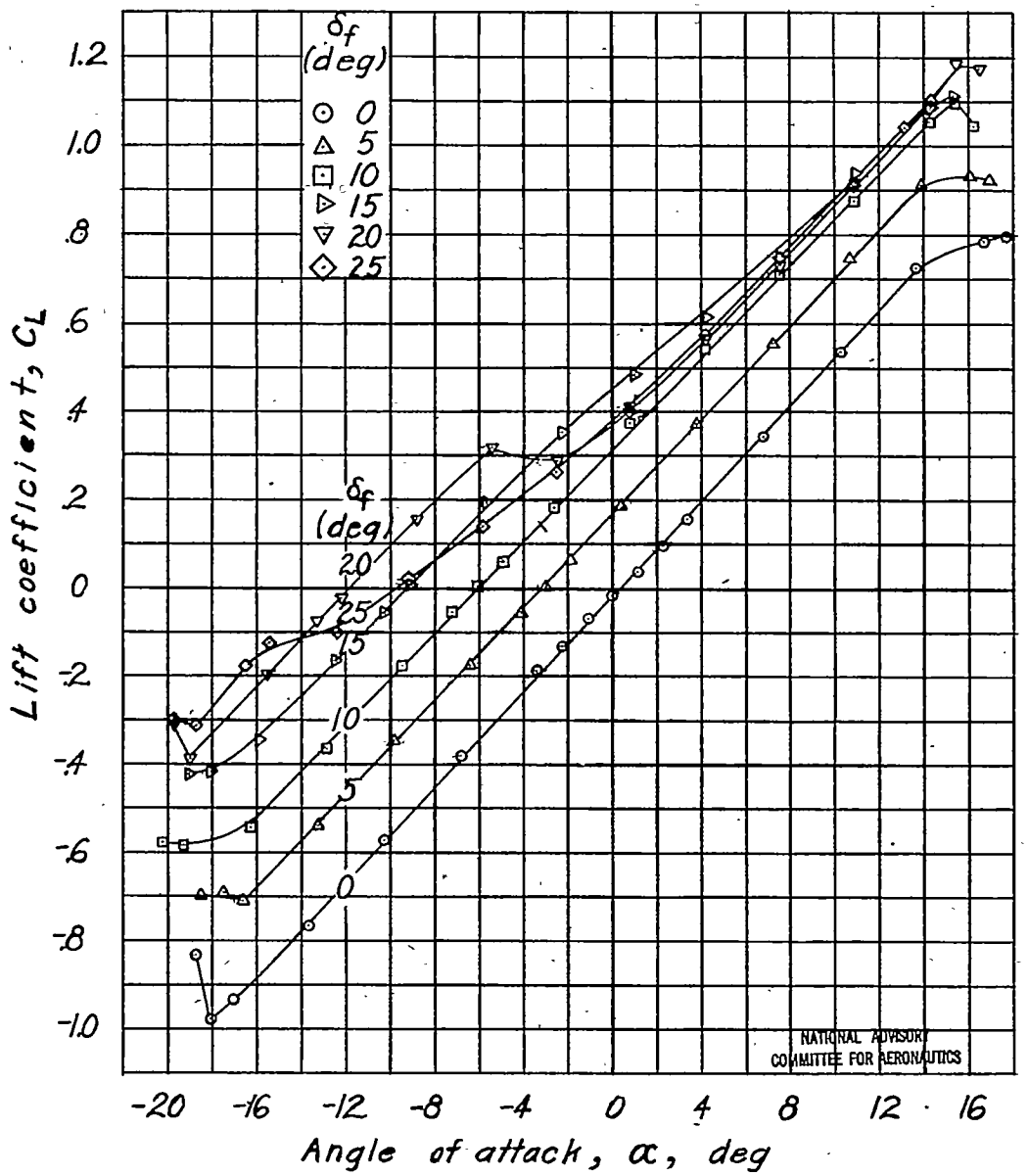

Figure 9.- Aerodynamic characteristics of a rectangular semispan tail surface. Flap with 0.50c_f blunt overhang; sealed gap; $\delta_t = 0°$; 0.30c flap; A=3.

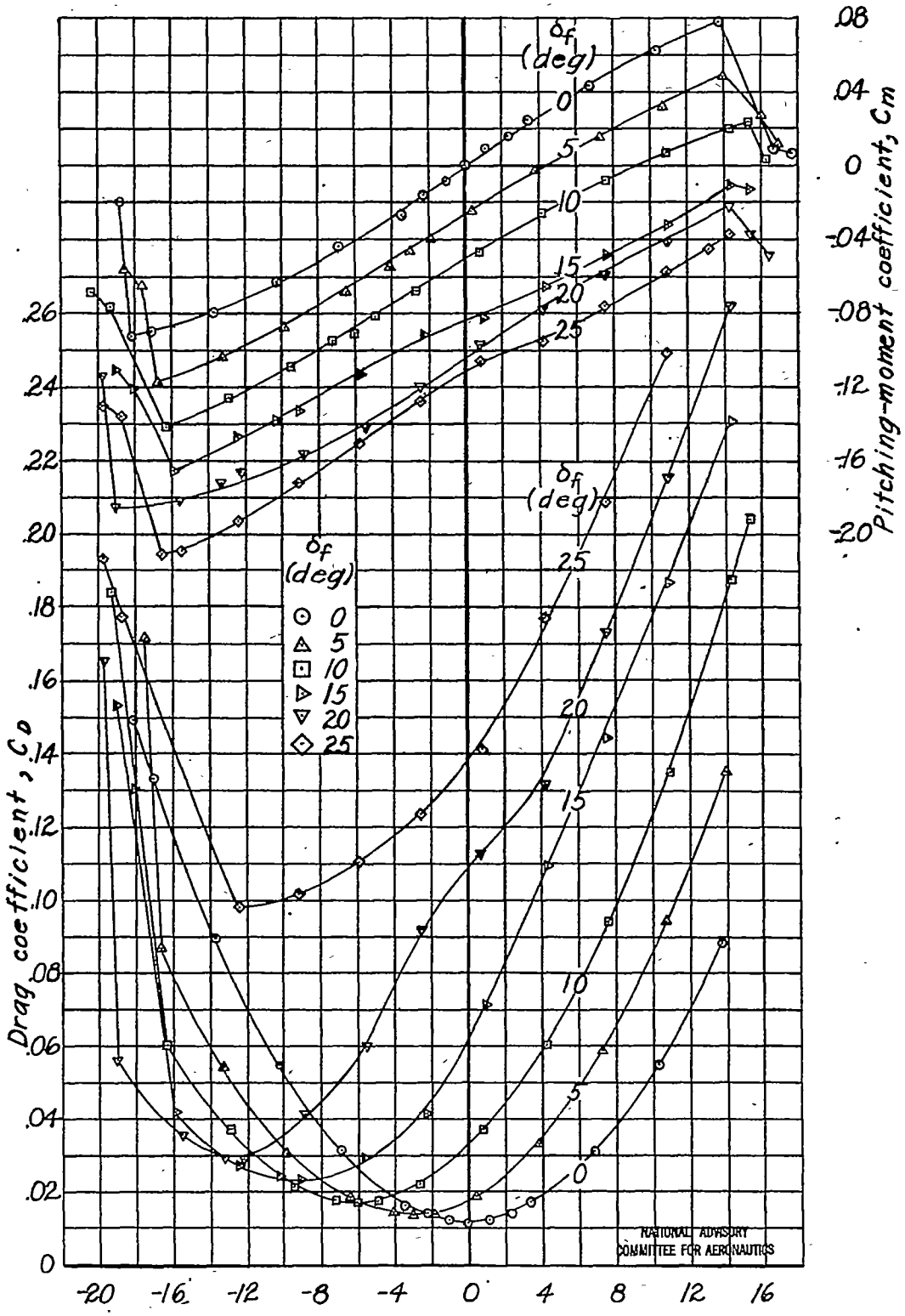

Figure 9.- Continued.

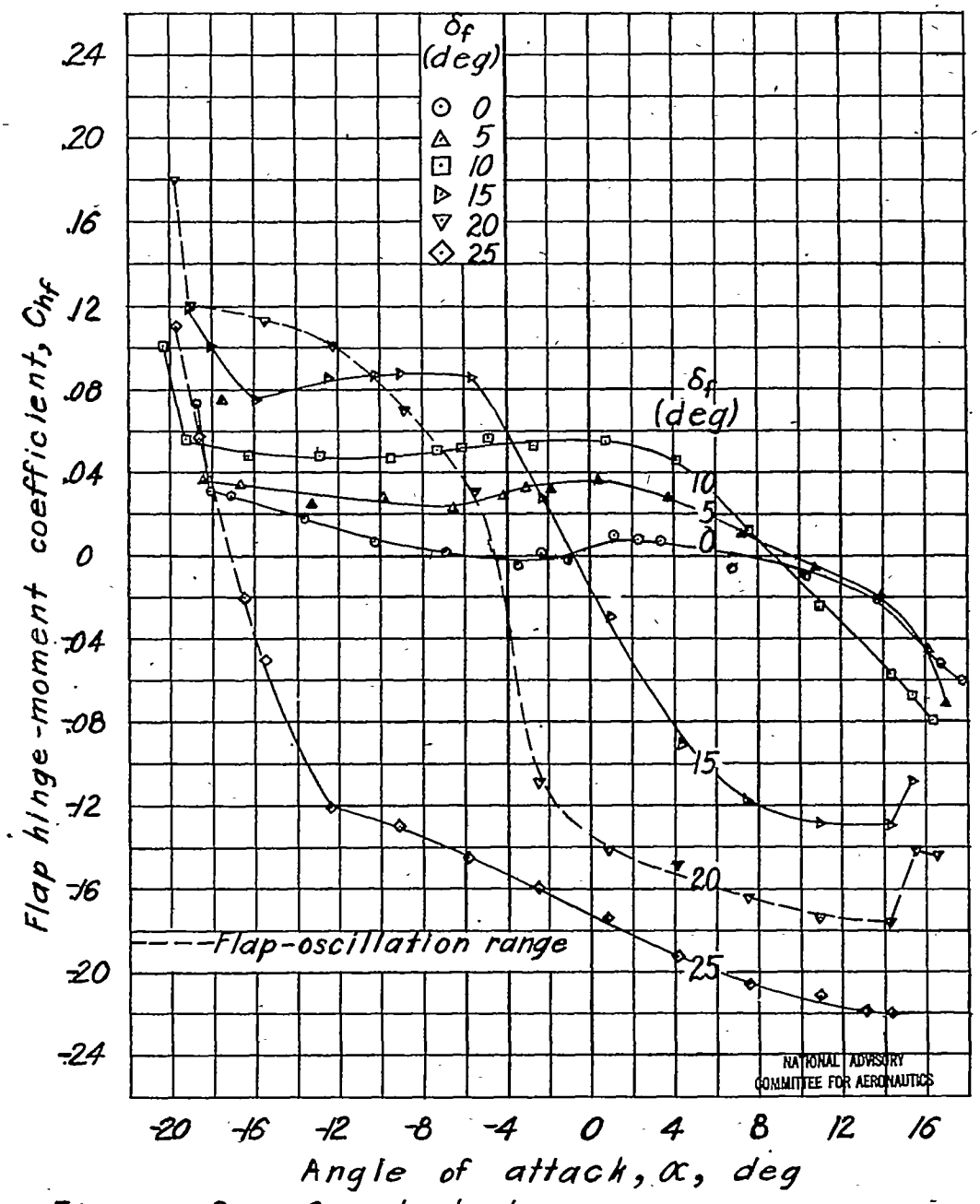

Figure 9.- Concluded.

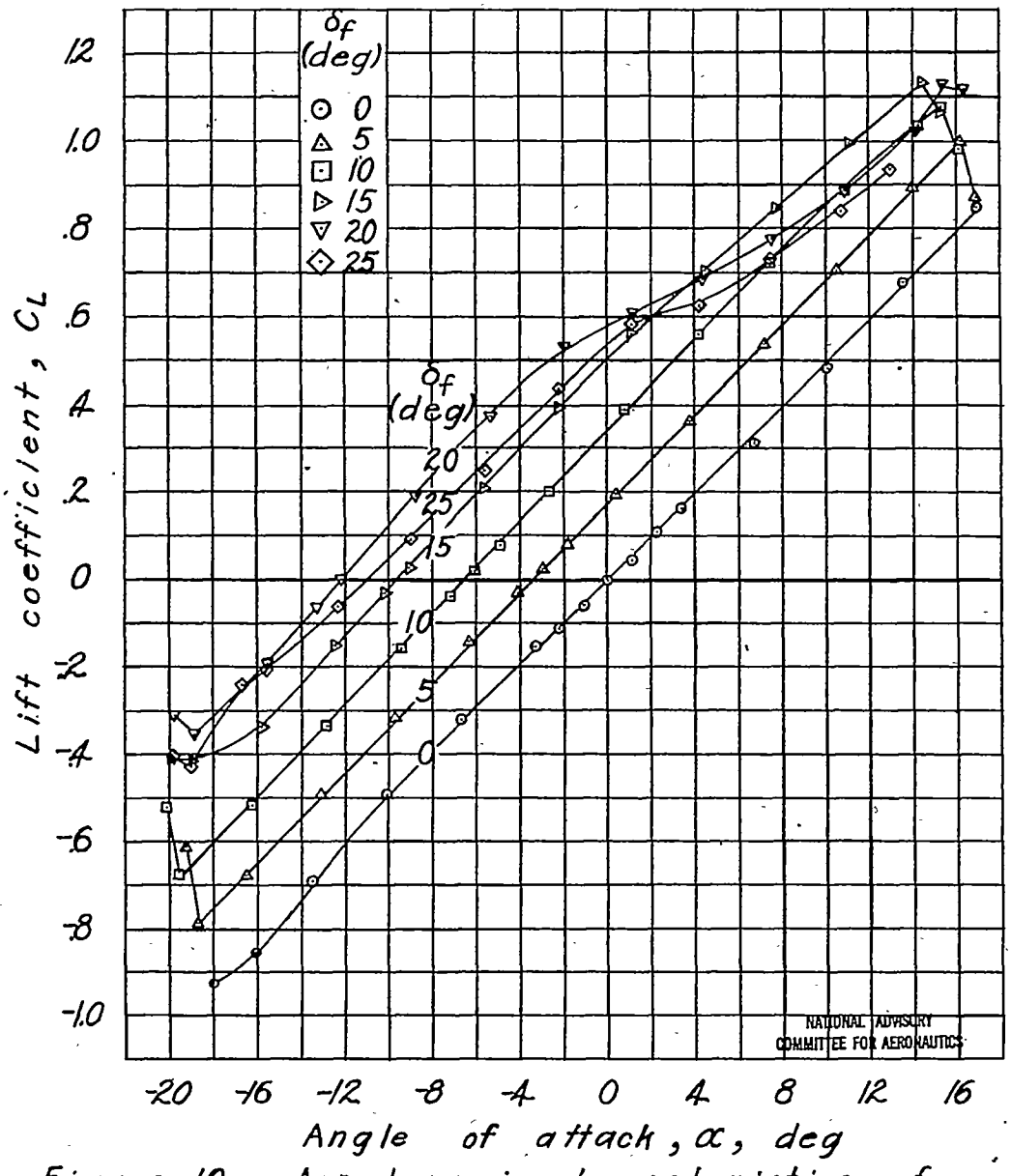

Figure 10.- Aerodynamic characteristics of a rectangular semispan tail surface. Flap with 0.50 c_f blunt overhang; 0.005c gap; $\delta_t = 0^\circ$; 0.30 c flap; A=3.

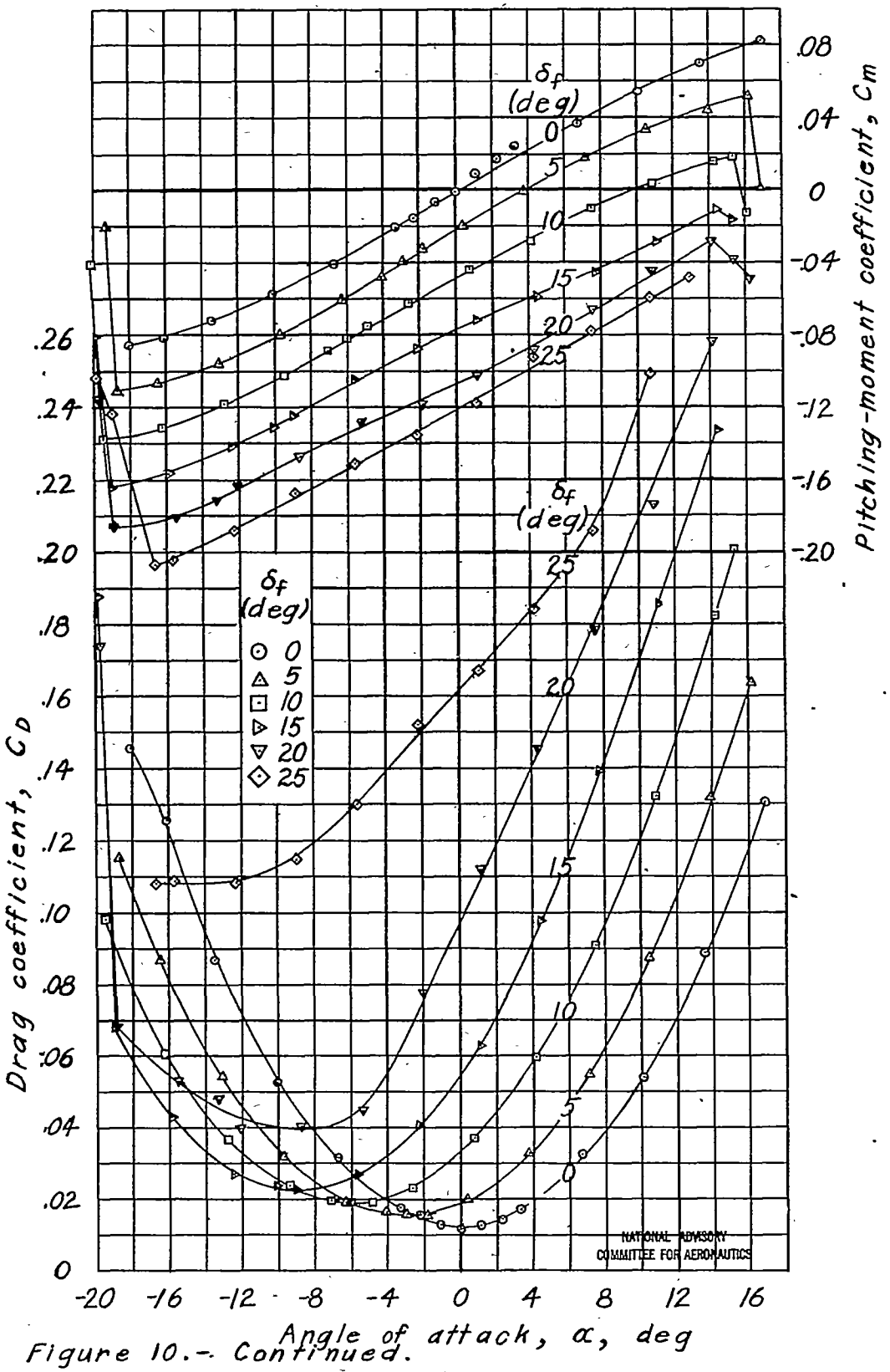

Figure 10.- Continued.

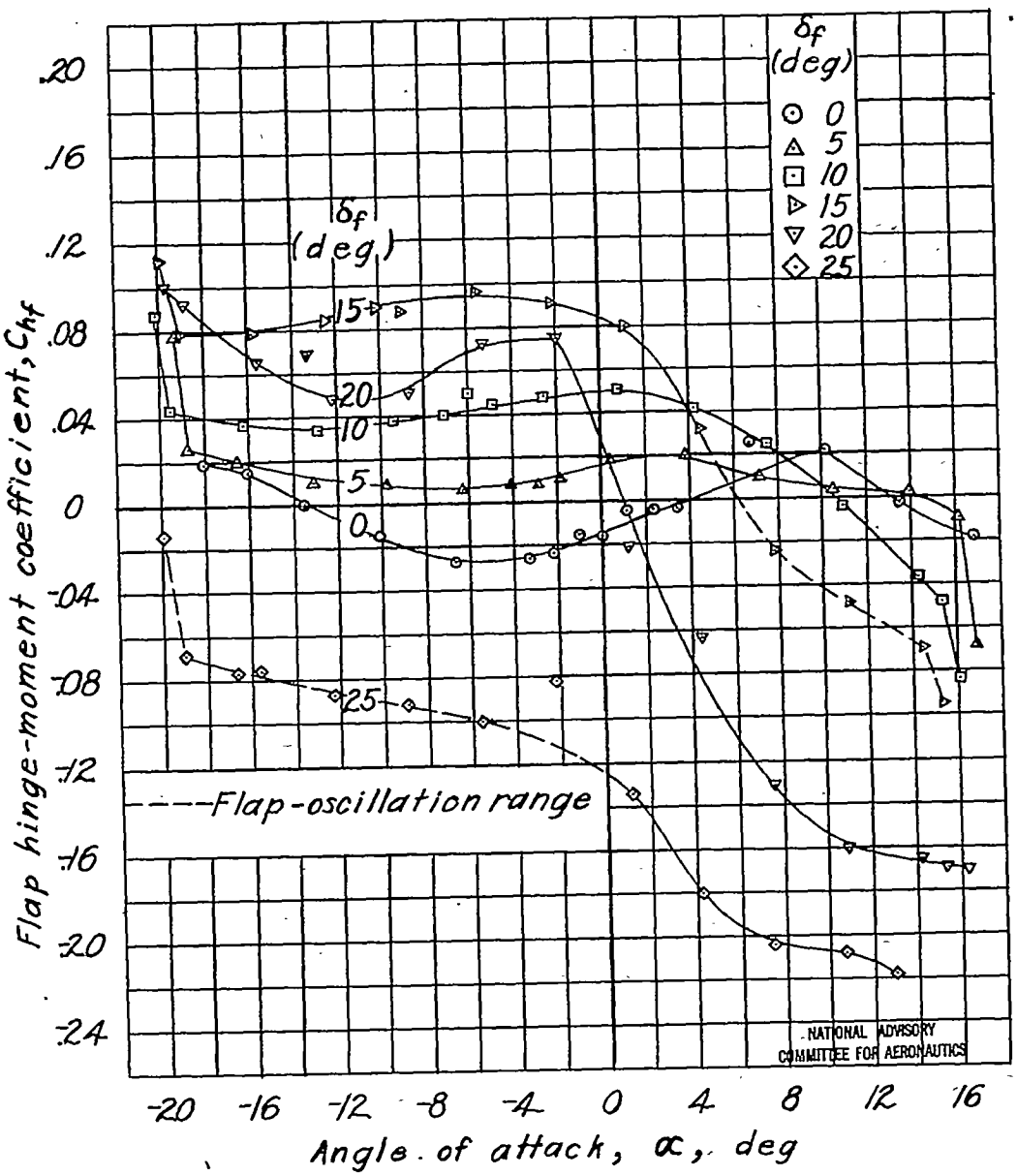

Figure 10.- Concluded.

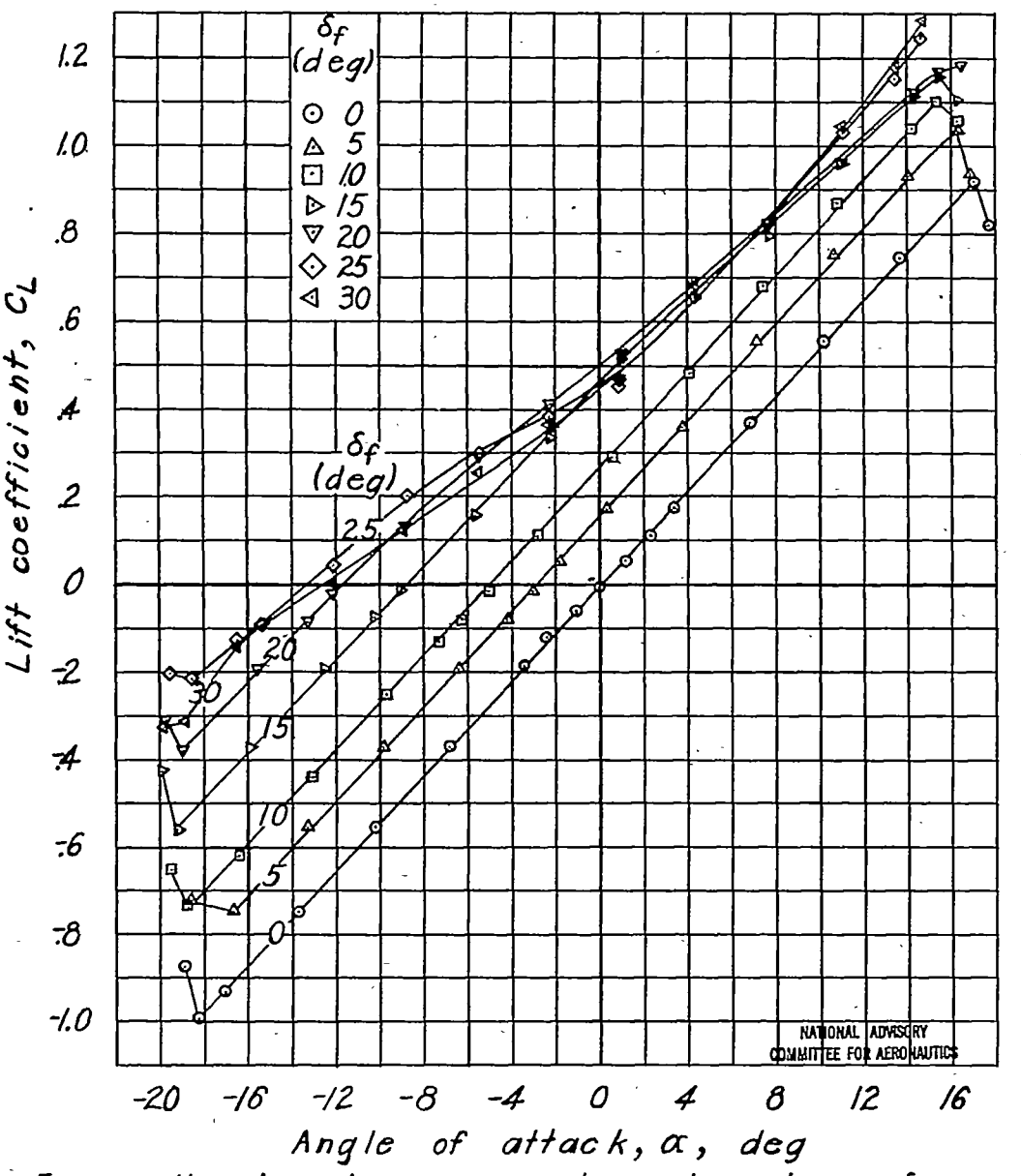

Figure 11.- Aerodynamic characteristics of a rectangular semispan tail surface. Flap with 0.50 c_f elliptical overhang; sealed gap; $\delta_t = 0^\circ$; 0.30 c flap; A=3.

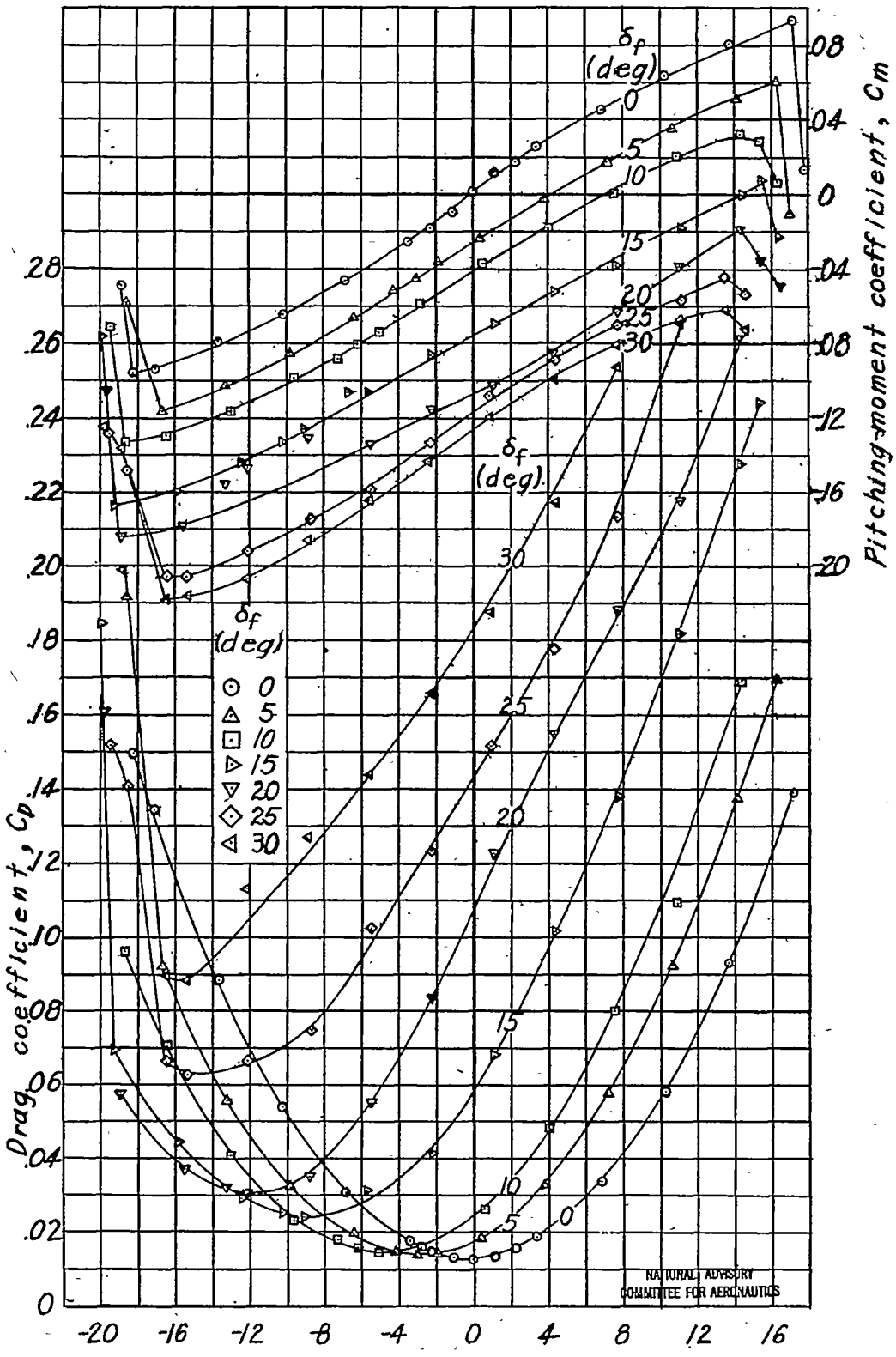

Figure 11.- Continued.

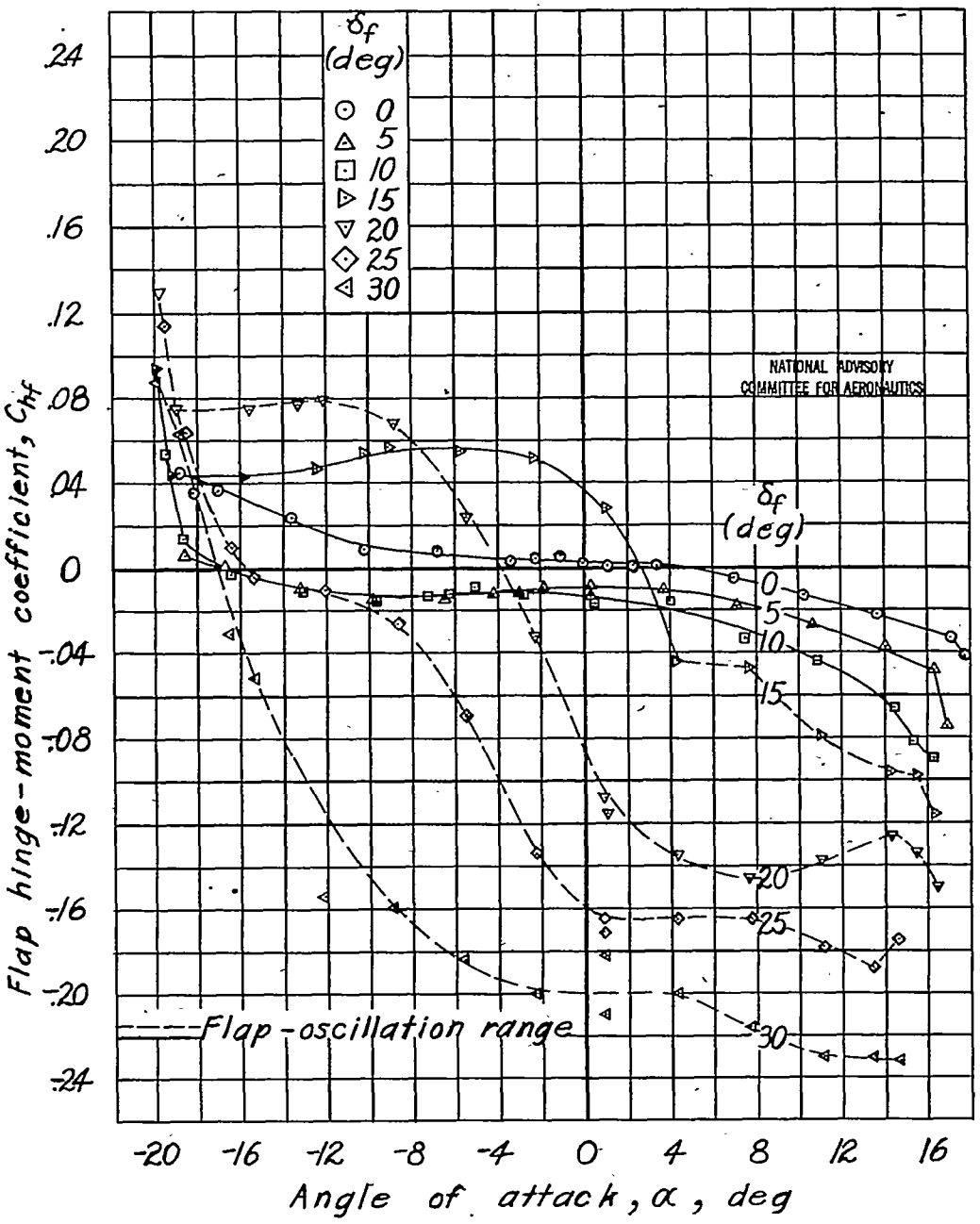

Figure 11.- Concluded.

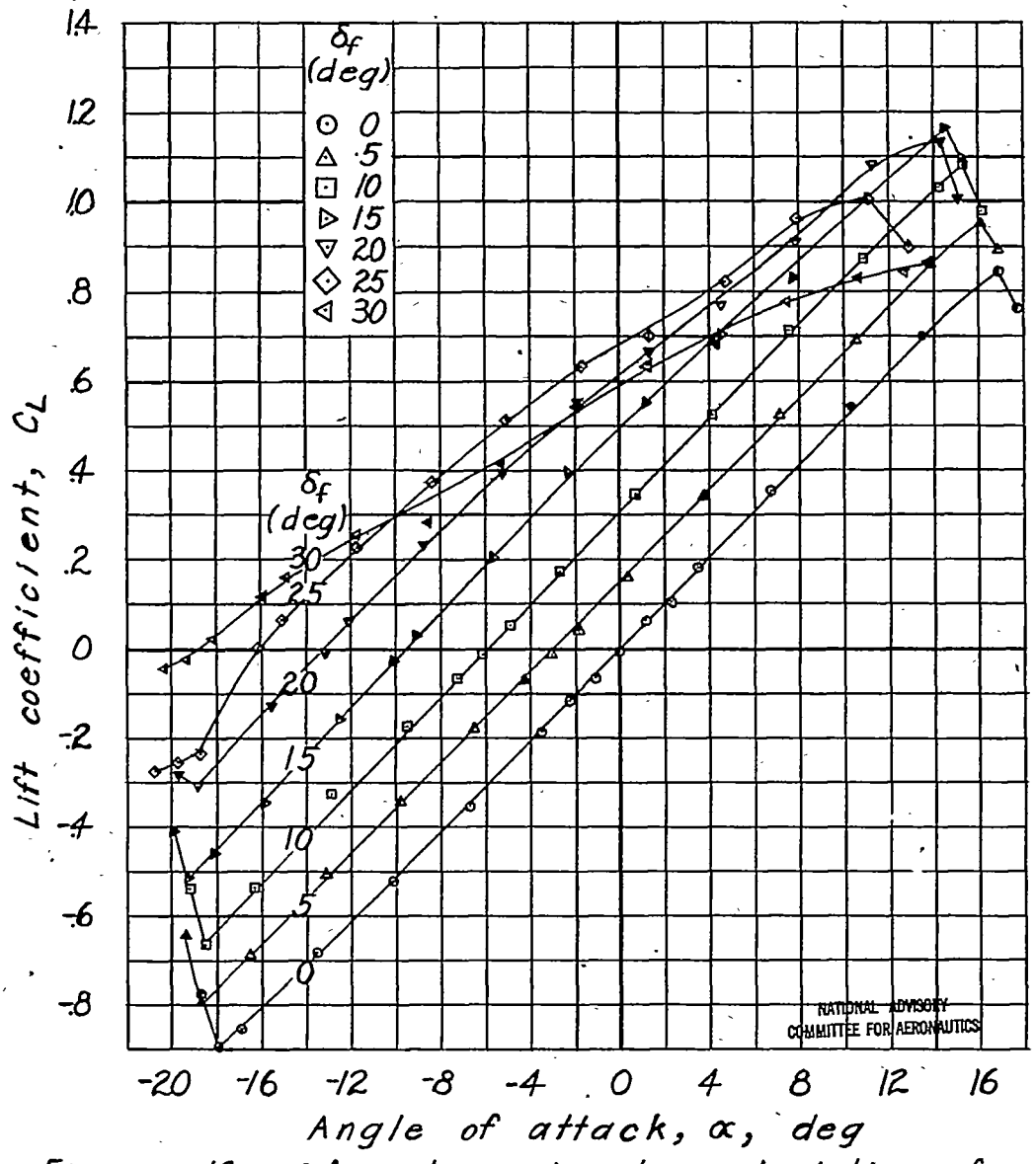

Figure 12.- Aerodynamic characteristics of a rectangular semispan tail surface. Flap with $0.50c_f$ elliptical overhang; $0.005c$ gap; $\delta_t = 0°$; $0.30c$ flap; $A = 3$.

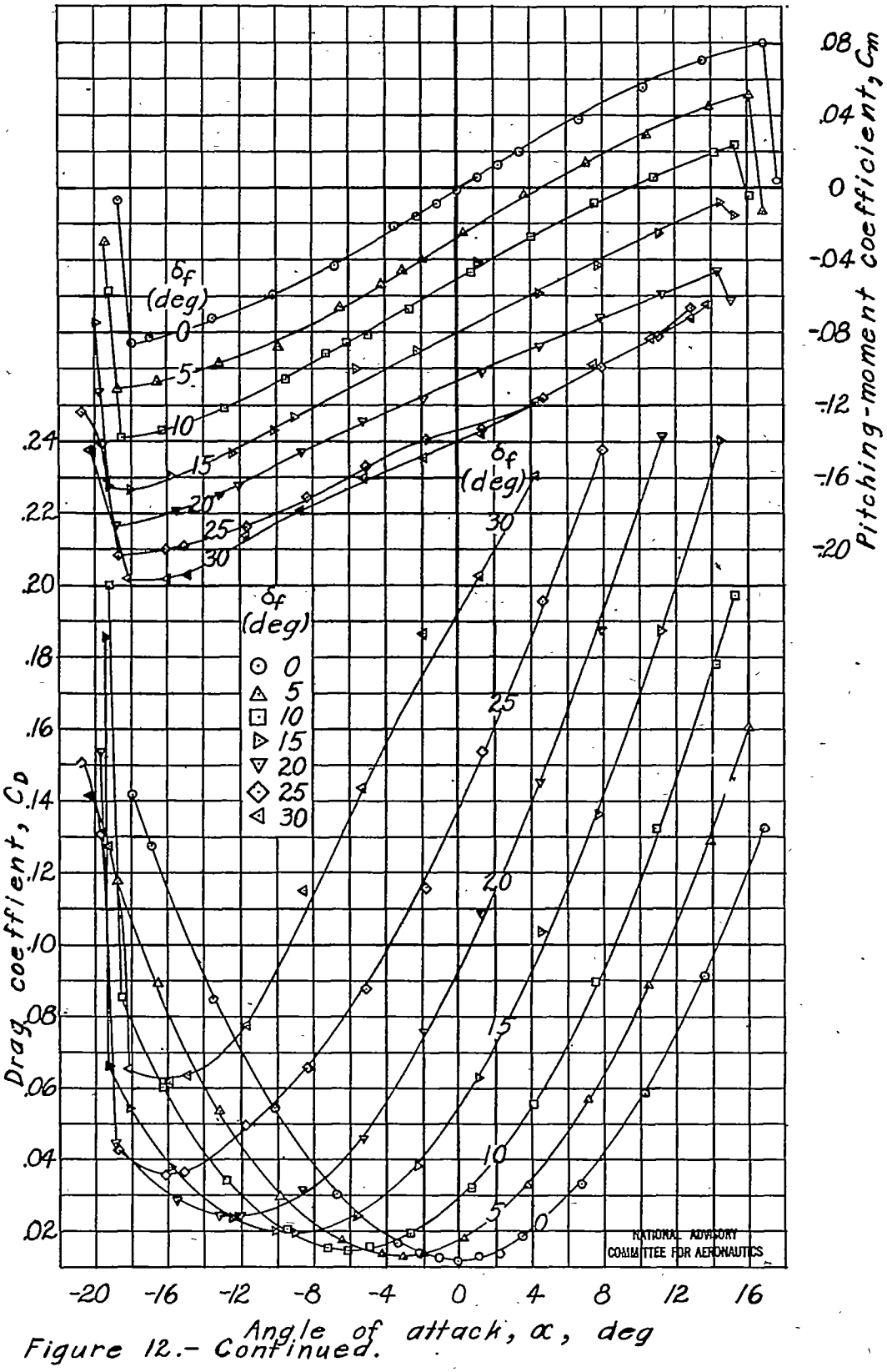

Figure 12.- Continued.

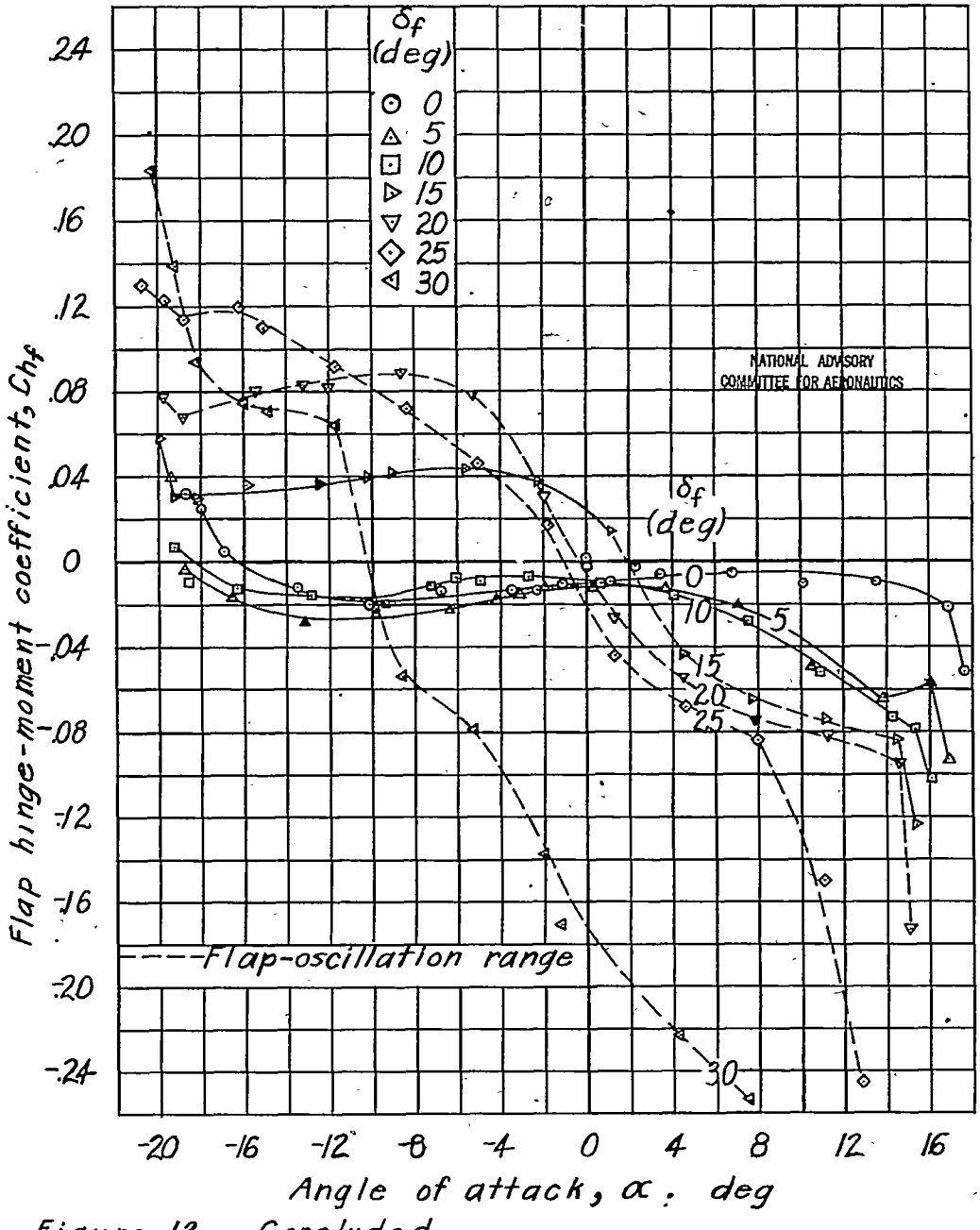

Figure 12.- Concluded.

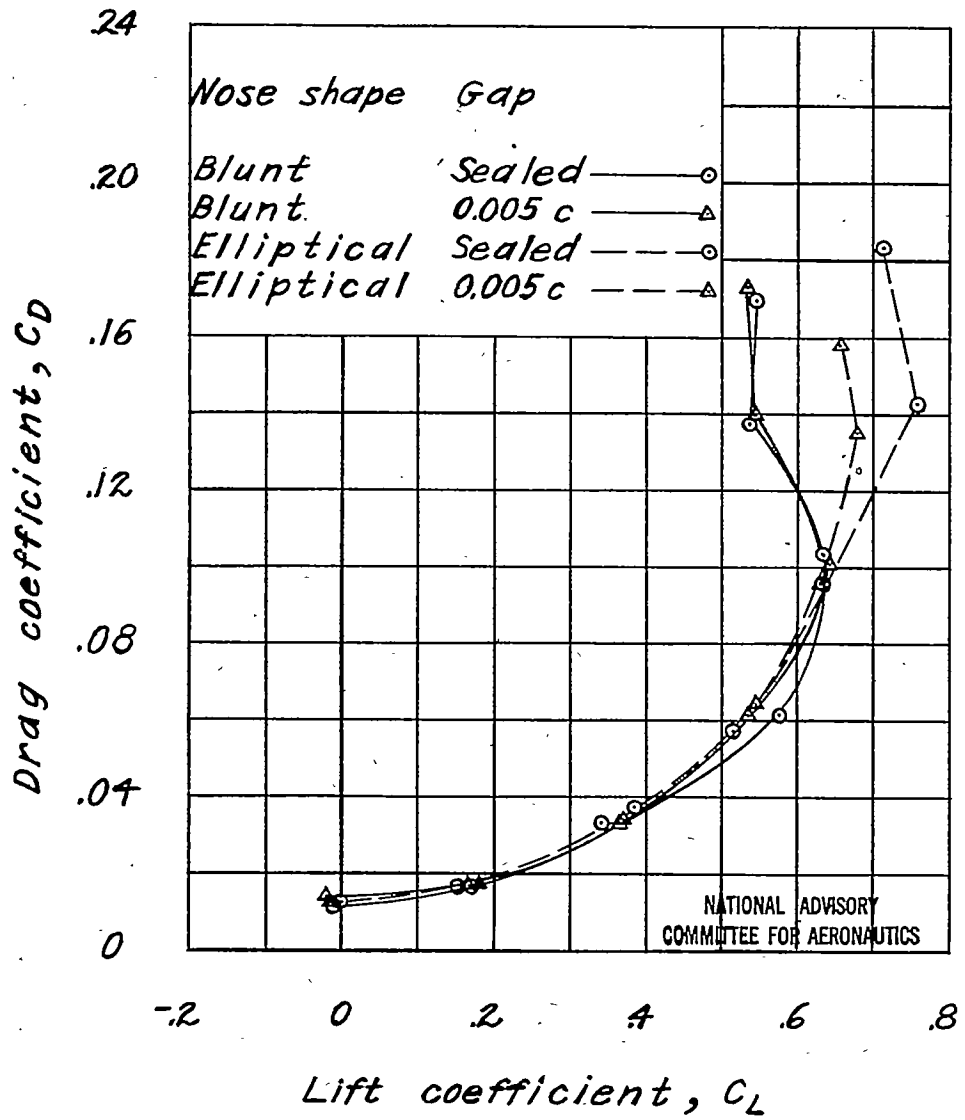

Figure 13.- Drag coefficient as a function of lift coefficient for a rectangular semispan tail surface with a 0.30c flap having a $0.35c_f$ overhang. $\alpha = 0°$; $A = 3$.

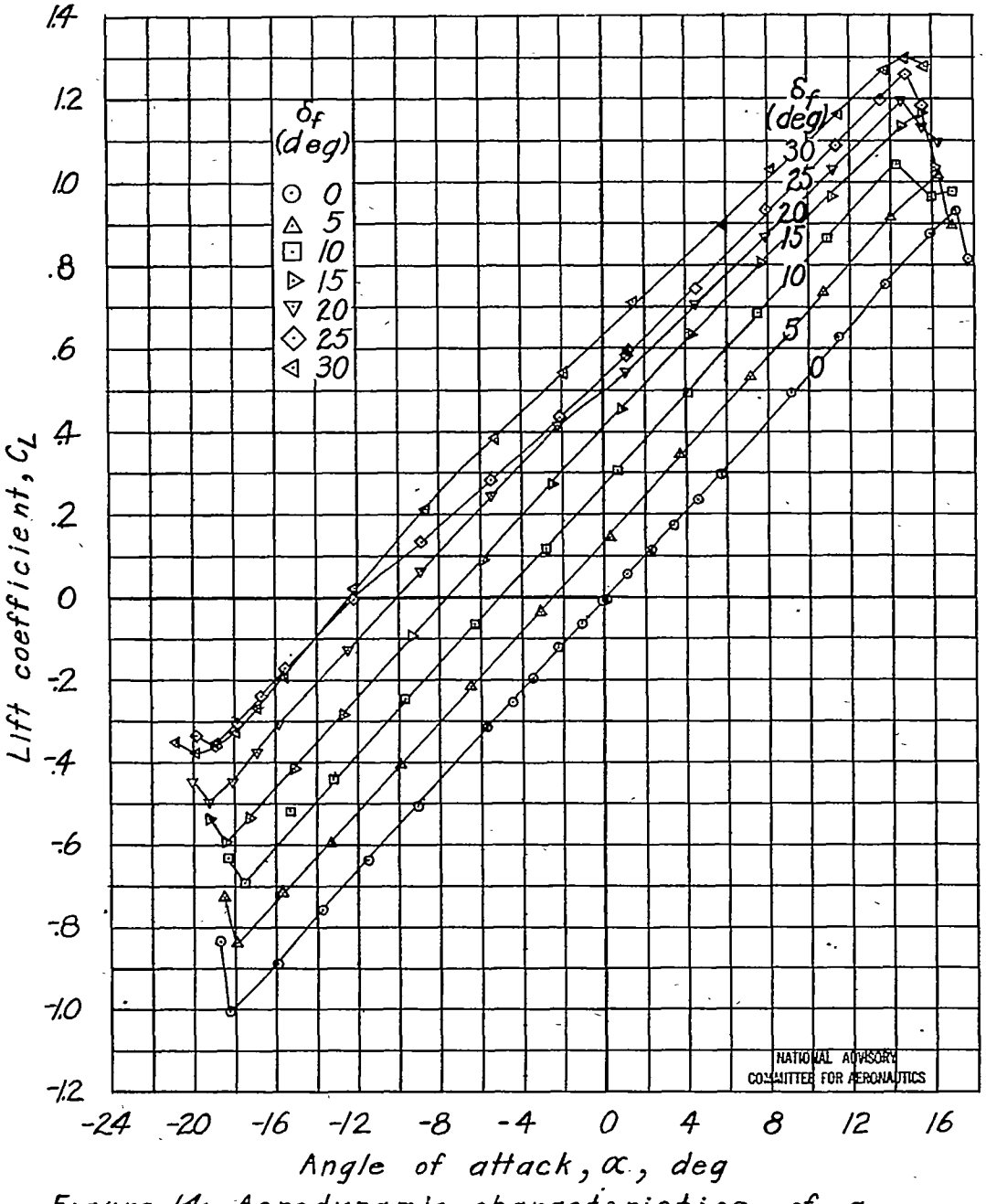

Figure 14.-Aerodynamic characteristics of a rectangular semispan tail surface. Plain flap; sealed gap; $\partial\delta_t/\partial\delta_f = -1$; 0.30c flap; A=3.

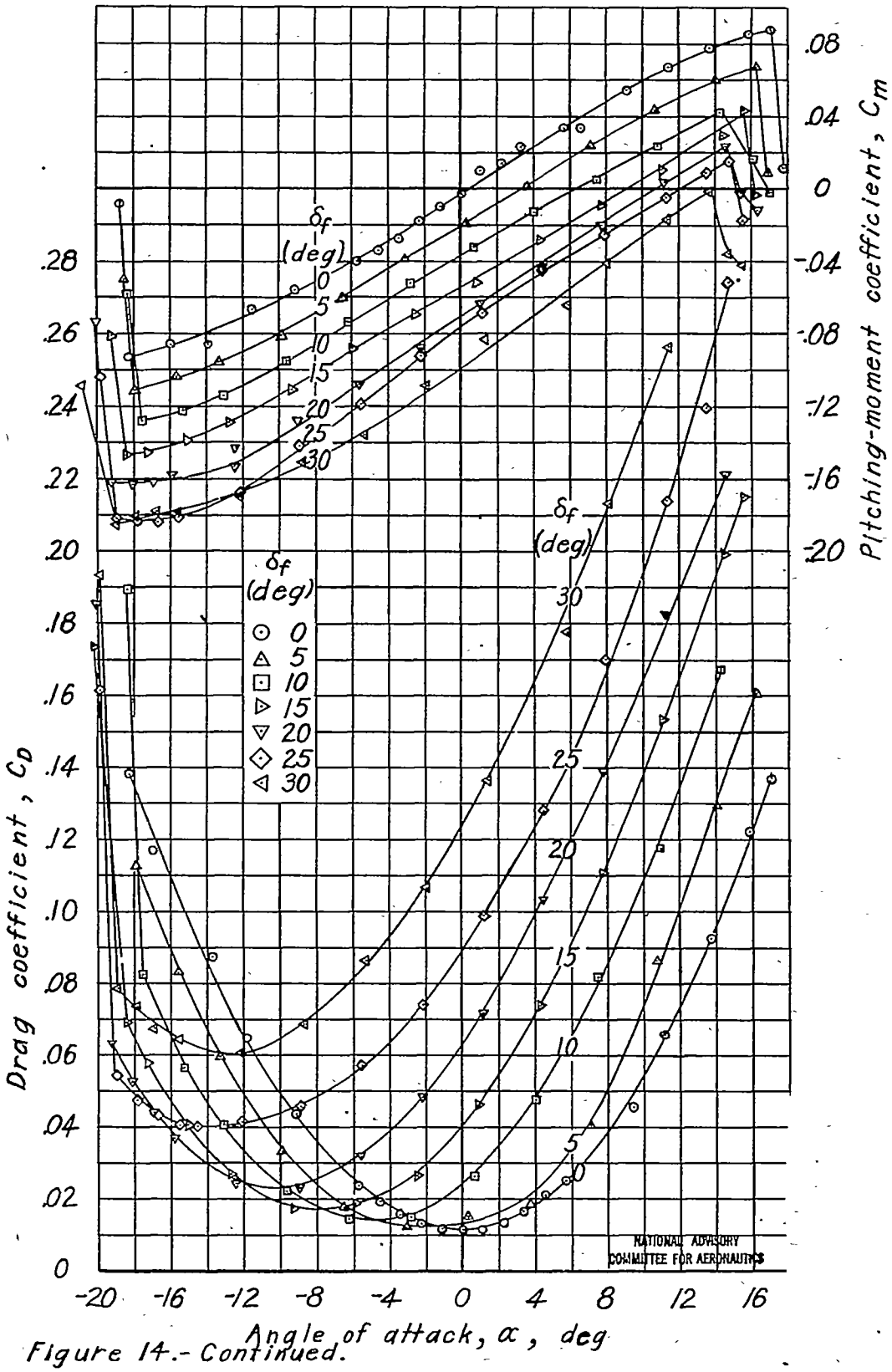

Figure 14.- Continued.

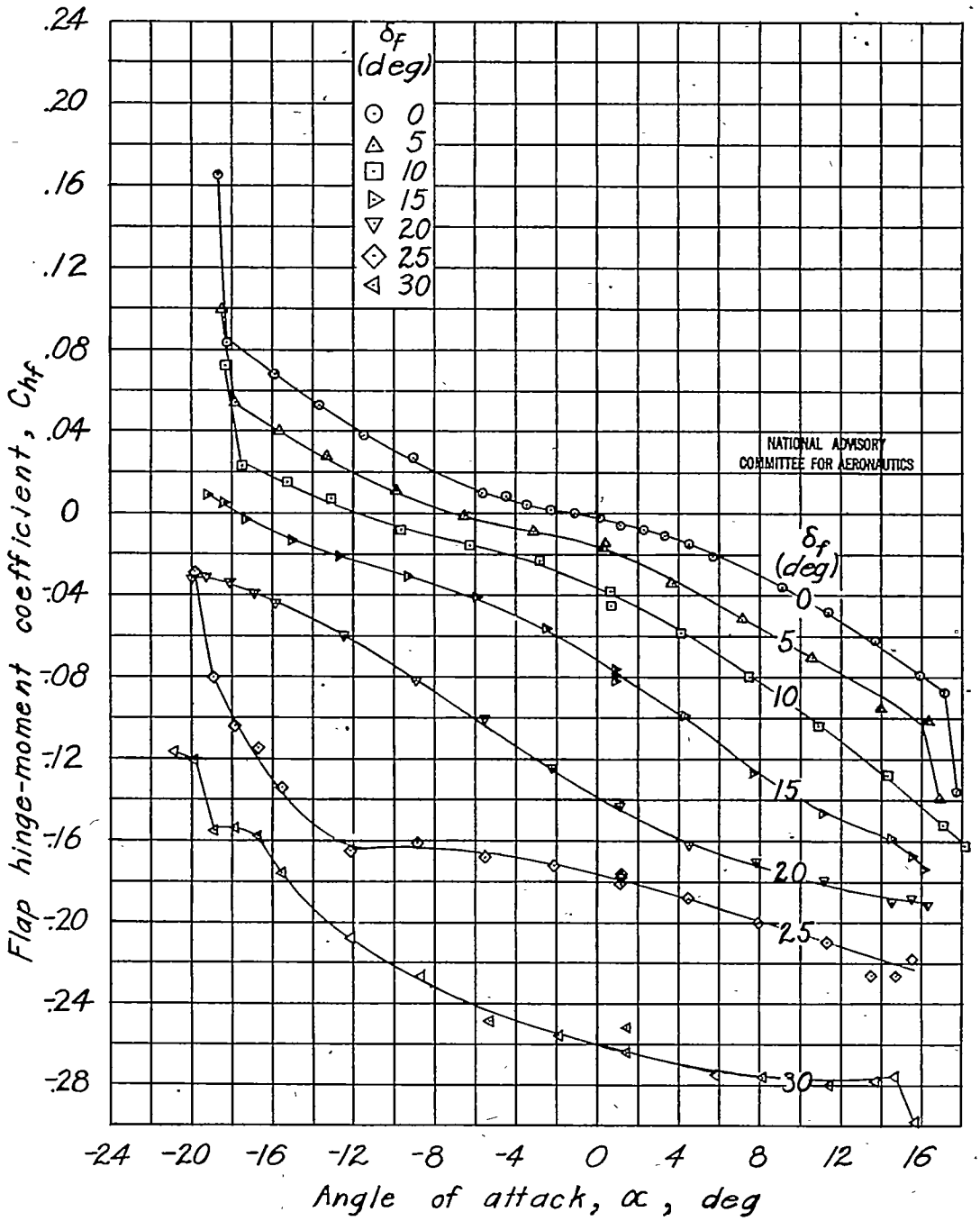

Figure 14.-Concluded.

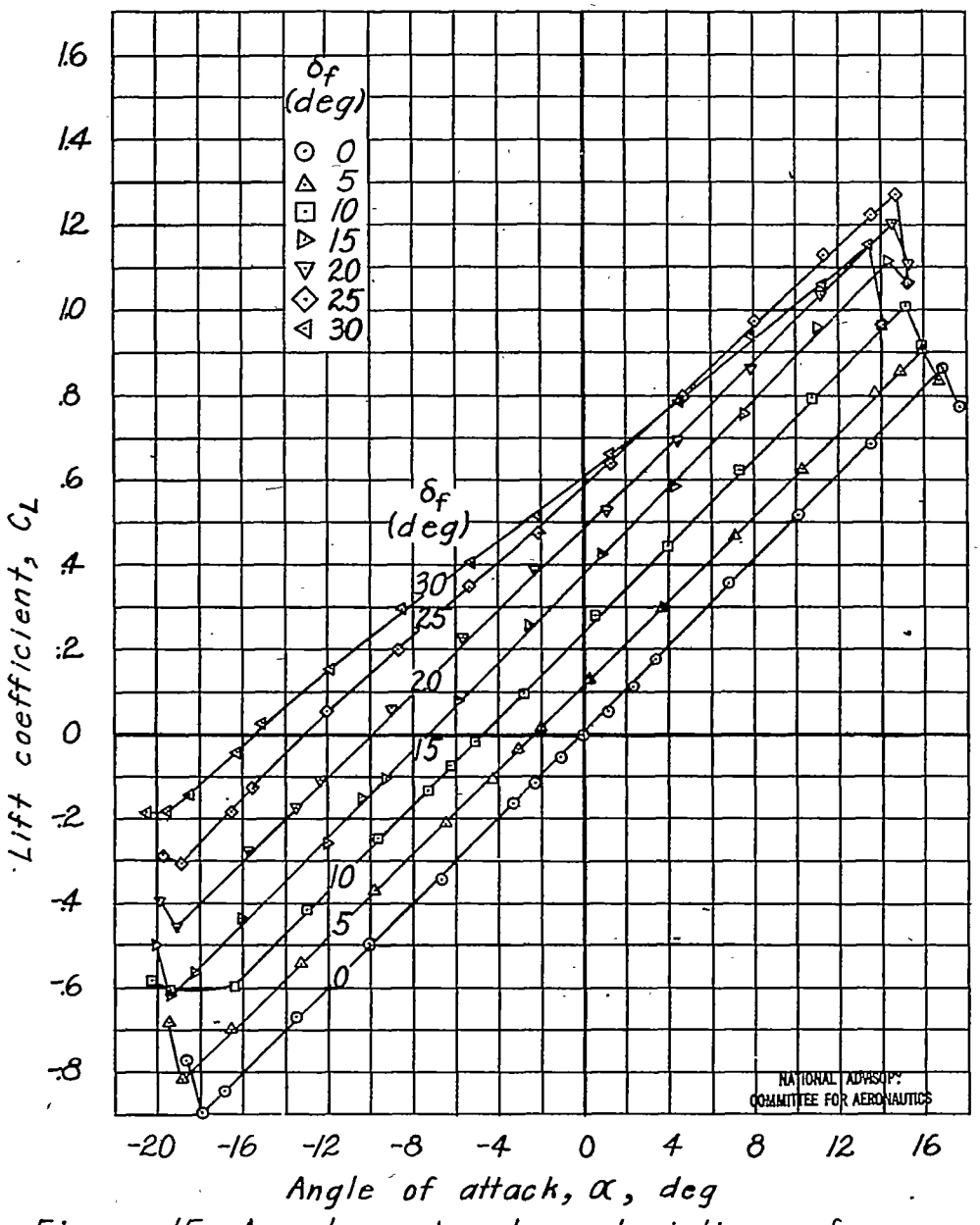

Figure 15.- Aerodynamic characteristics of a rectangular semispan tail surface. Flap with $0.35c_f$ elliptical overhang; 0.005c gap; $\partial\delta_t/\partial\delta_f = -1$; 0.30c flap; A=3.

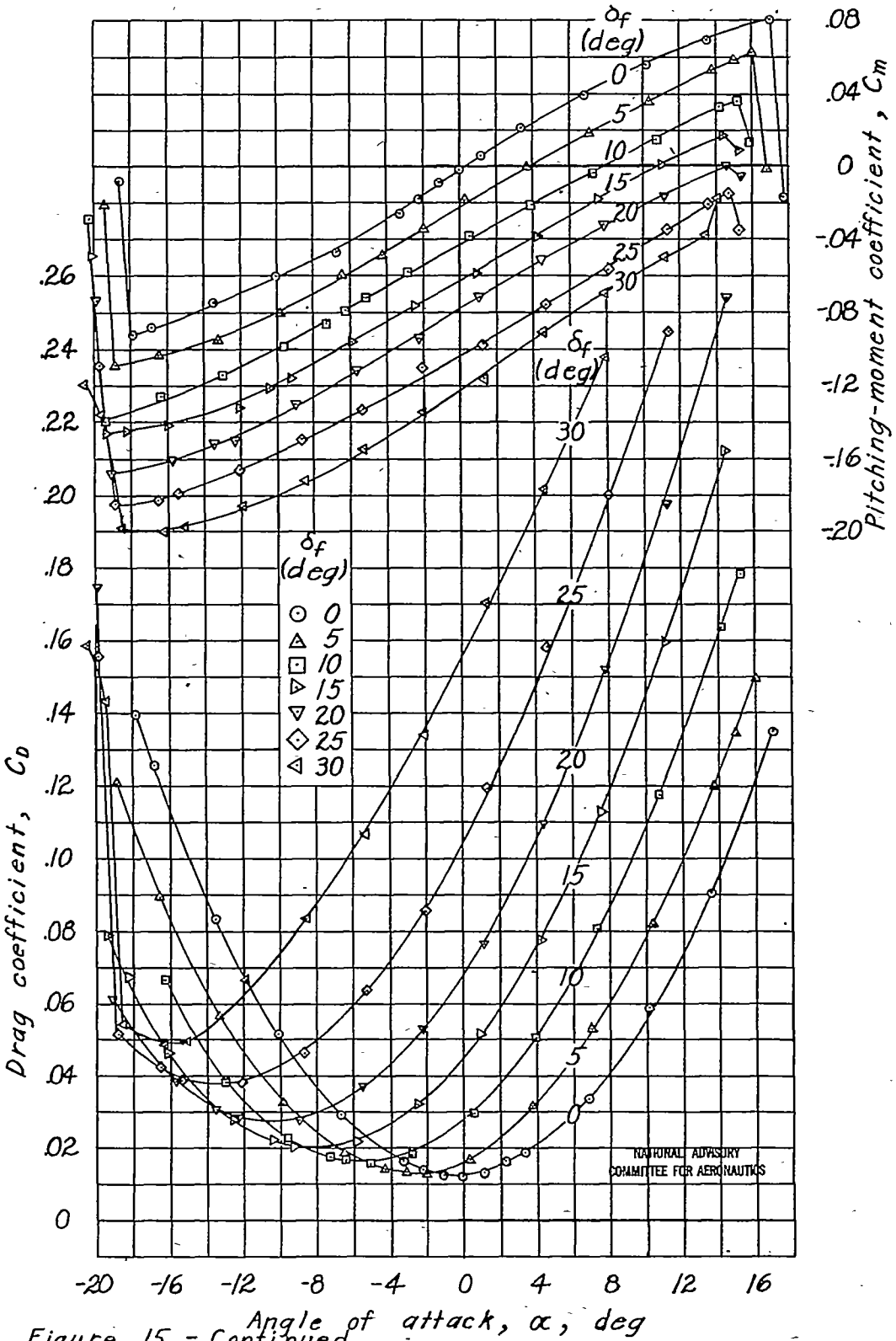

Figure 15.- Continued.

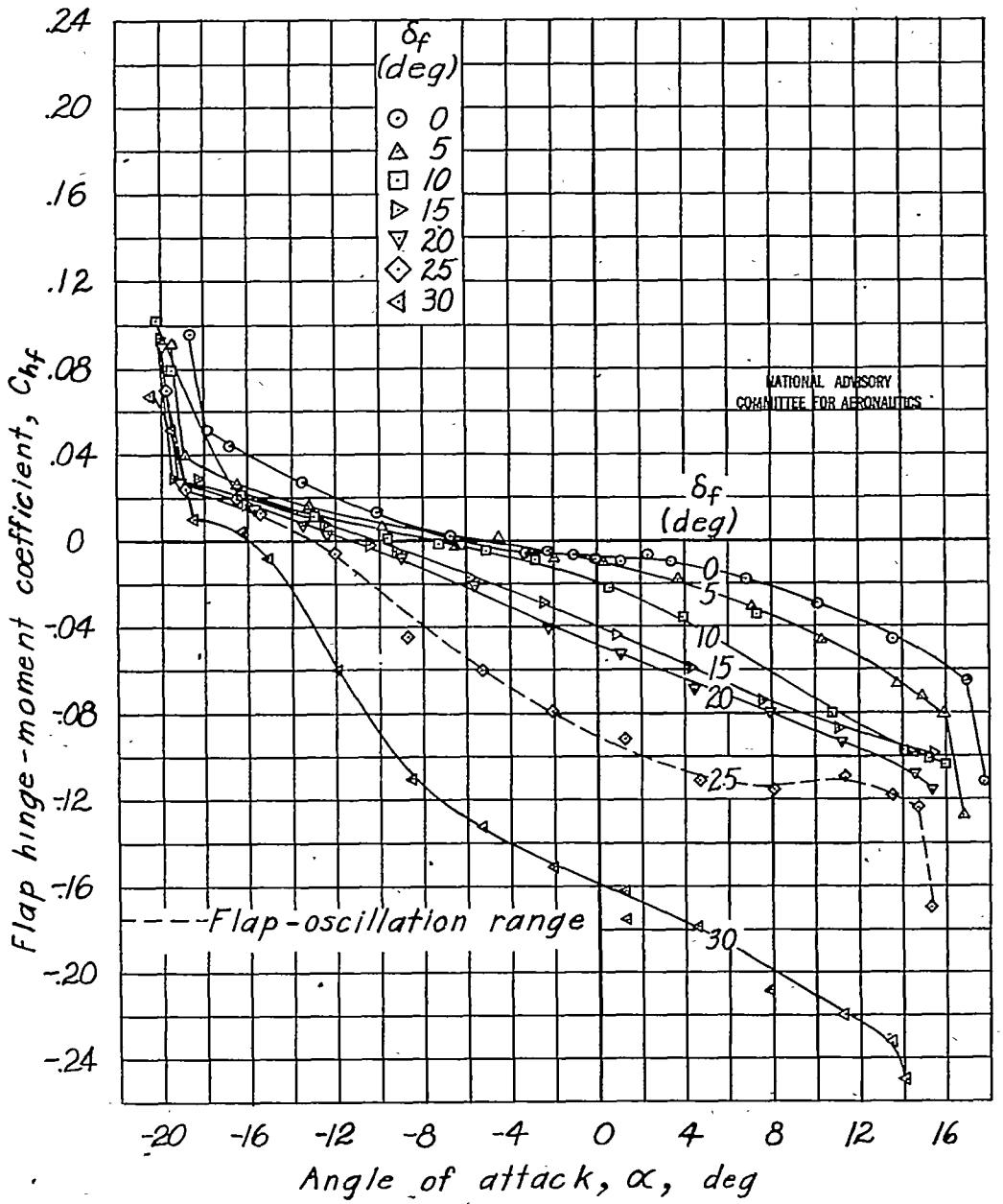

Figure 15.- Concluded.

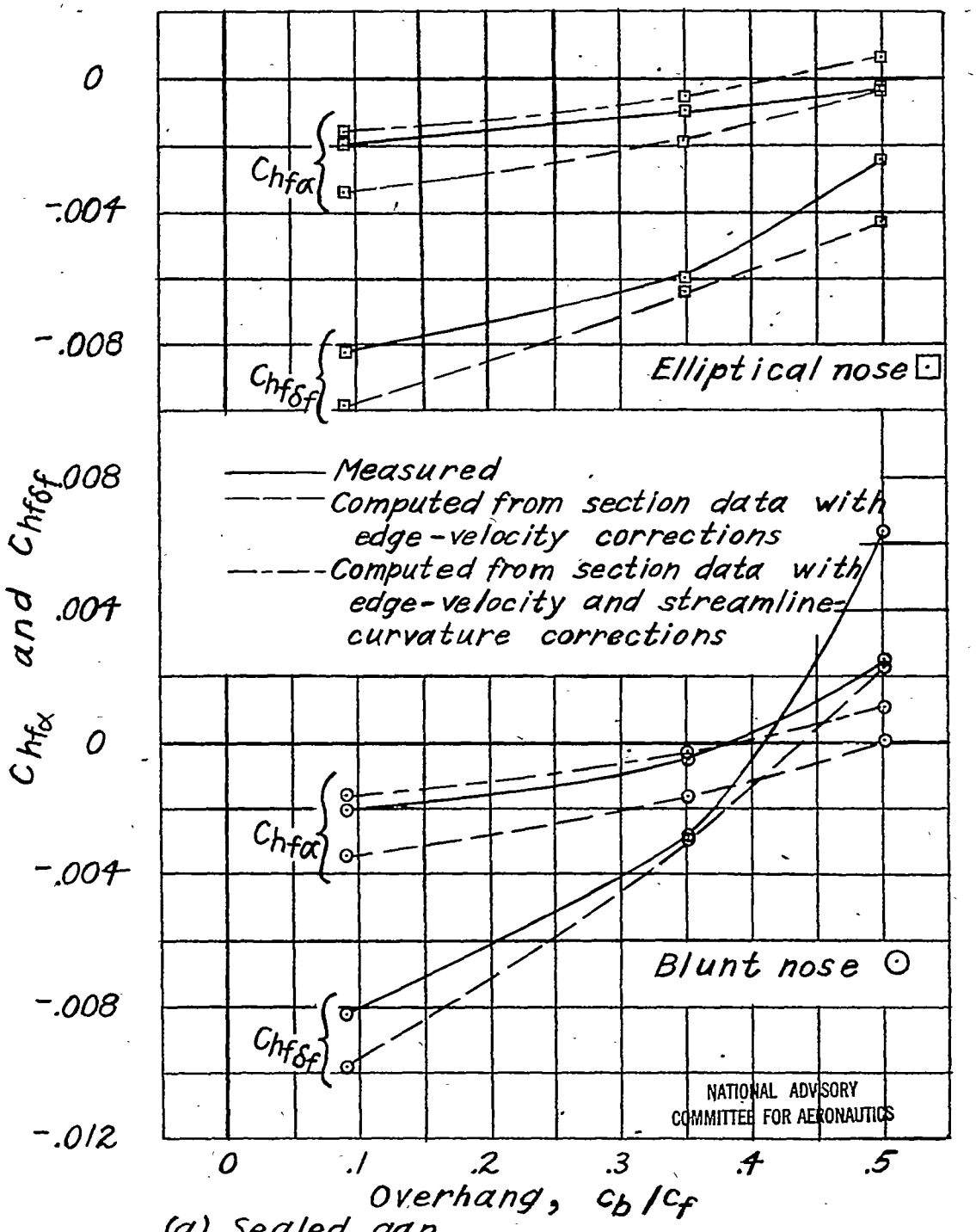

(a) Sealed gap.

Figure 16.- Variation of flap hinge-moment parameters with overhang for a rectangular semispan tail surface. 0.30c flap; A=3.

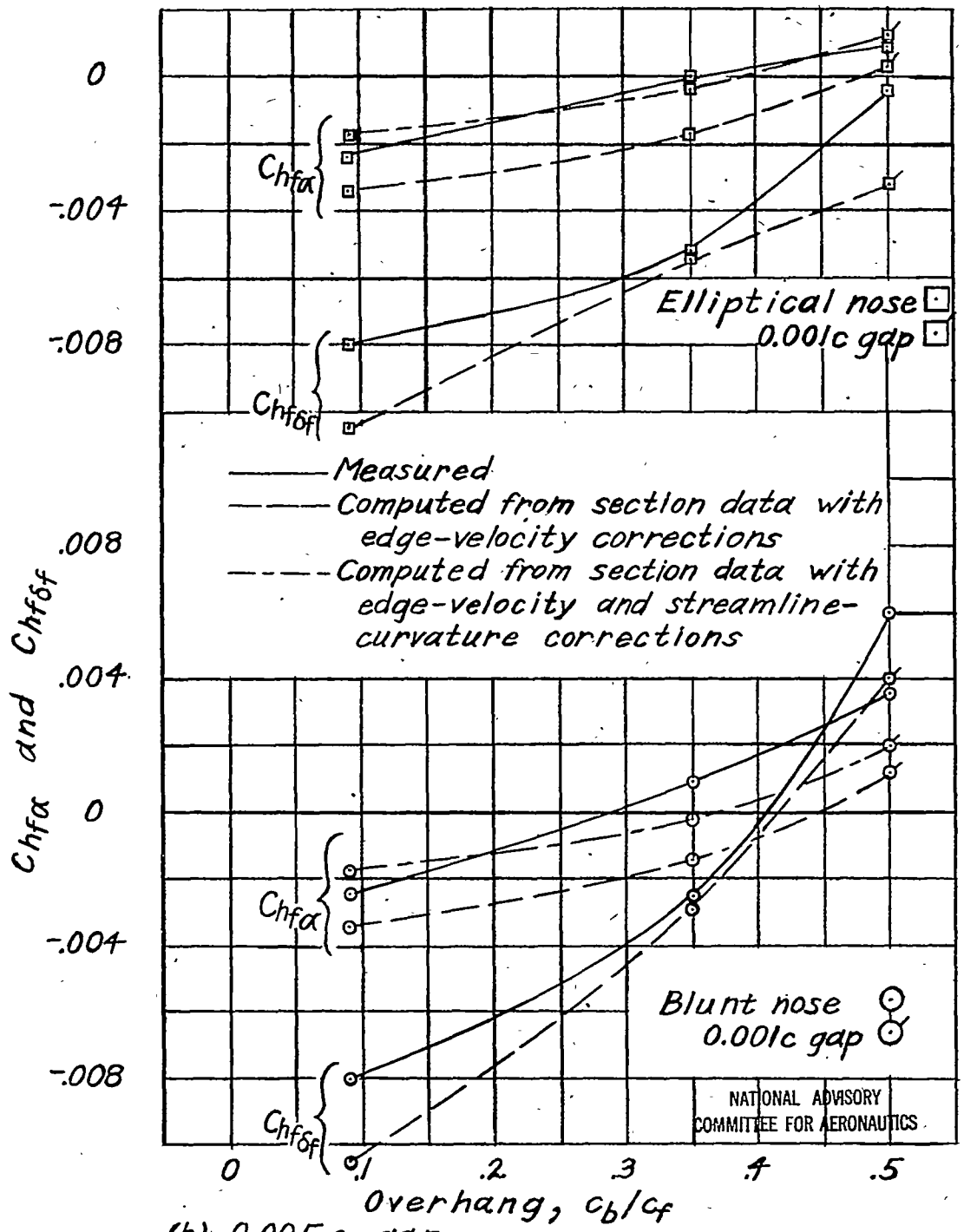

(b) 0.005c gap.

Figure 16.- Concluded.